MPI@LHC 2023
Manchester, November 23th, 2023

Results on forward particle production and energy flow at the LHC

Oscar Adriani
University of Florence & INFN Firenze

- Main focus on LHCf data
- Some highlight from ATLAS and CMS

Why forward physics@LHC is important (from the point of view of a Cosmic Ray physicist 😉)

Ultra High Energy Cosmic Rays

Studying the properties of primary High Energy Cosmic Rays based on observation of EAS

- X_{max} : depth of air shower maximum in the atmosphere
- RMS(X_{max}): fluctuations in the position of the shower maximum
- N_{μ}: number of muons in the shower at the detector level

+

MC Simulation to describe hadronic interaction with atmosphere

Energy, mass composition, direction
—> source of primary cosmic rays
—> origin of the universe (final goal)

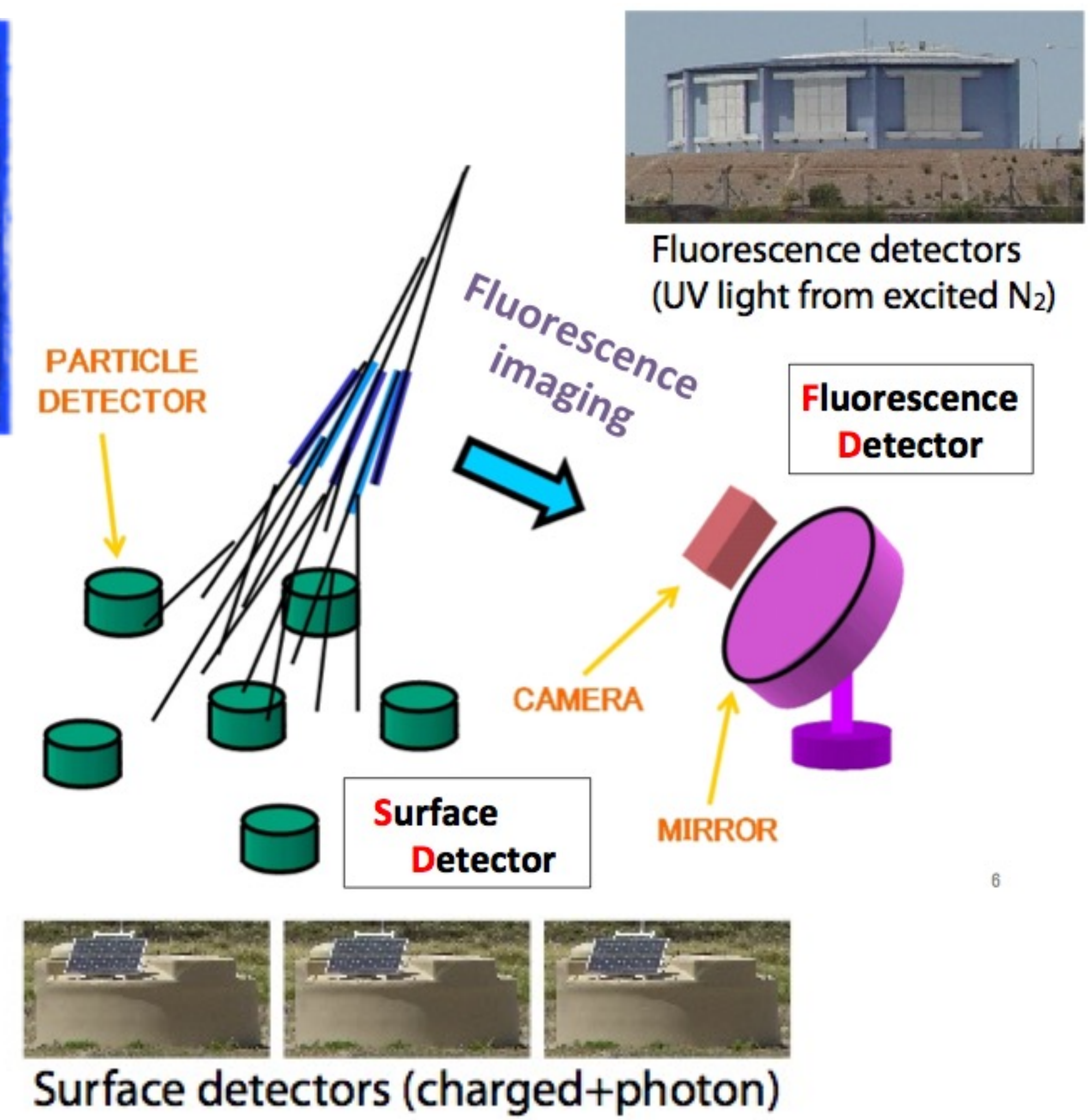

How accelerator experiments can contribute?

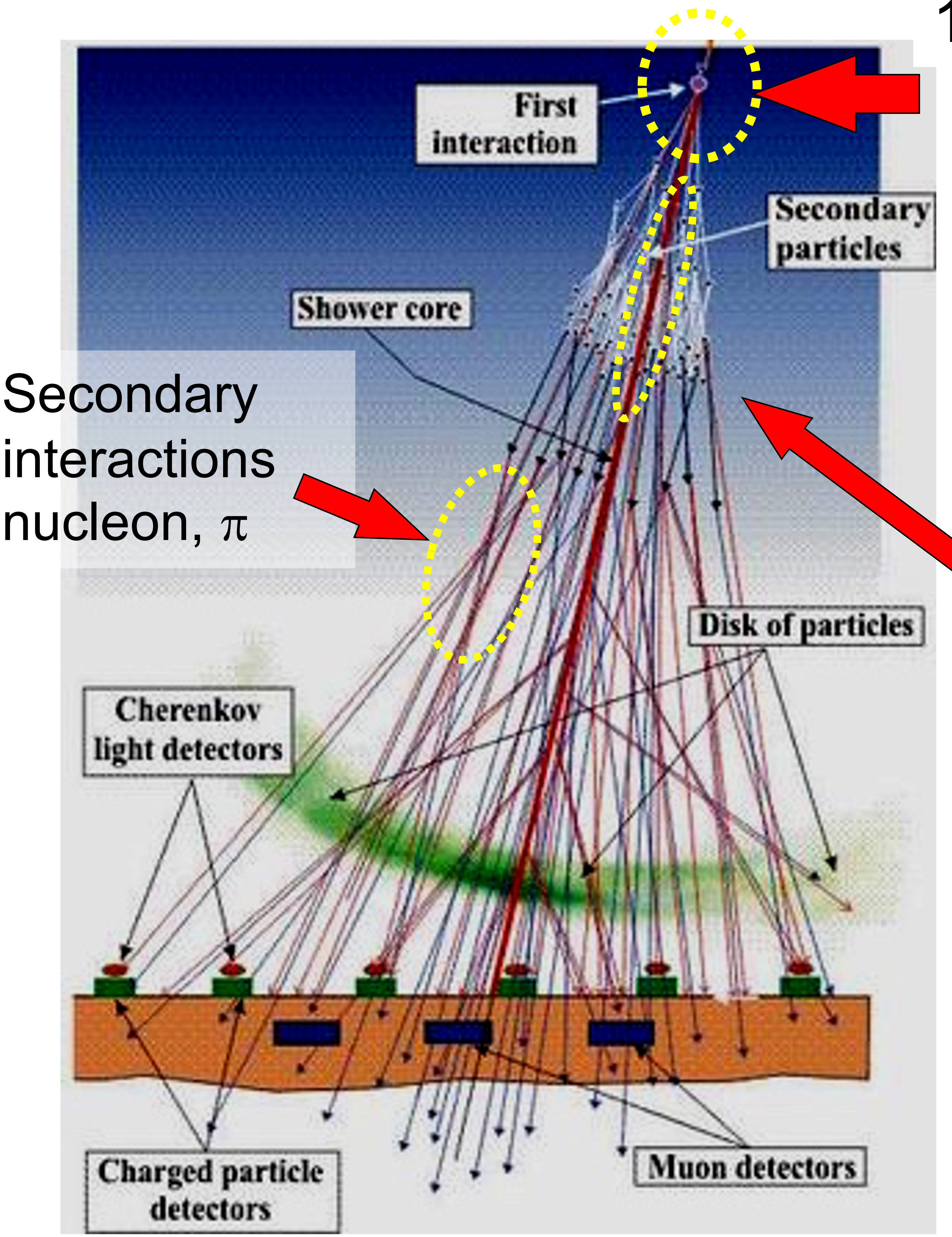

1. Inelastic cross section

If large σ: rapid development If small σ: deep penetrating

2. Multiplicity

If large: rapid development If small: deep penetrating

Totem, Atlas, CMS…

3. **Forward energy spectrum**

If softer shallow development If harder deep penetrating

4. **Inelasticity $k=1-E_{lead}/E_{avail}$**

If large k (π^0s carry more energy) rapid development If small k (baryons carry more energy) deep penetrating

5. **Nuclear Effect (p-Nucleus)**

LHCf

Spectrum of cosmic rays

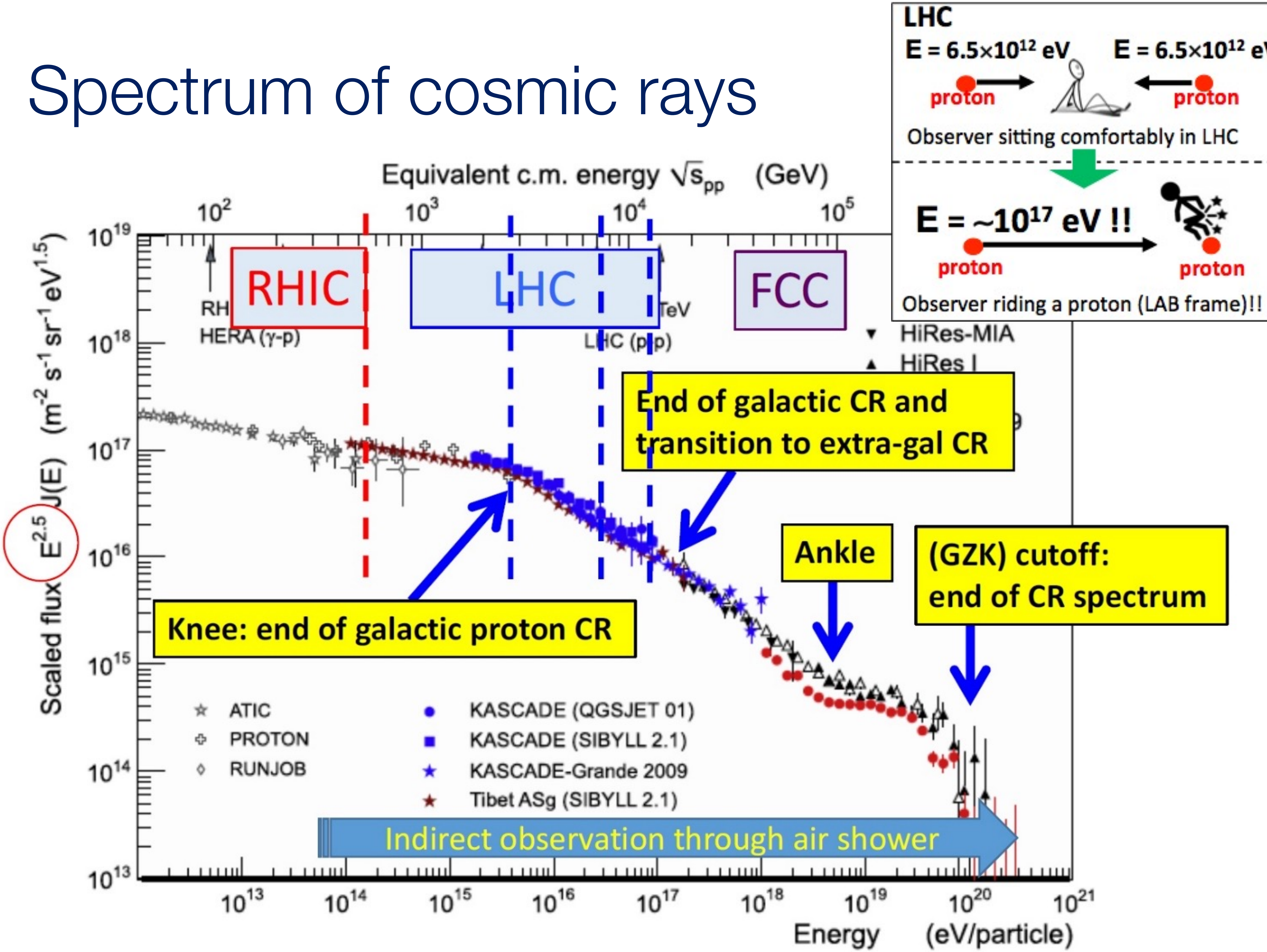

LHC phase space coverage

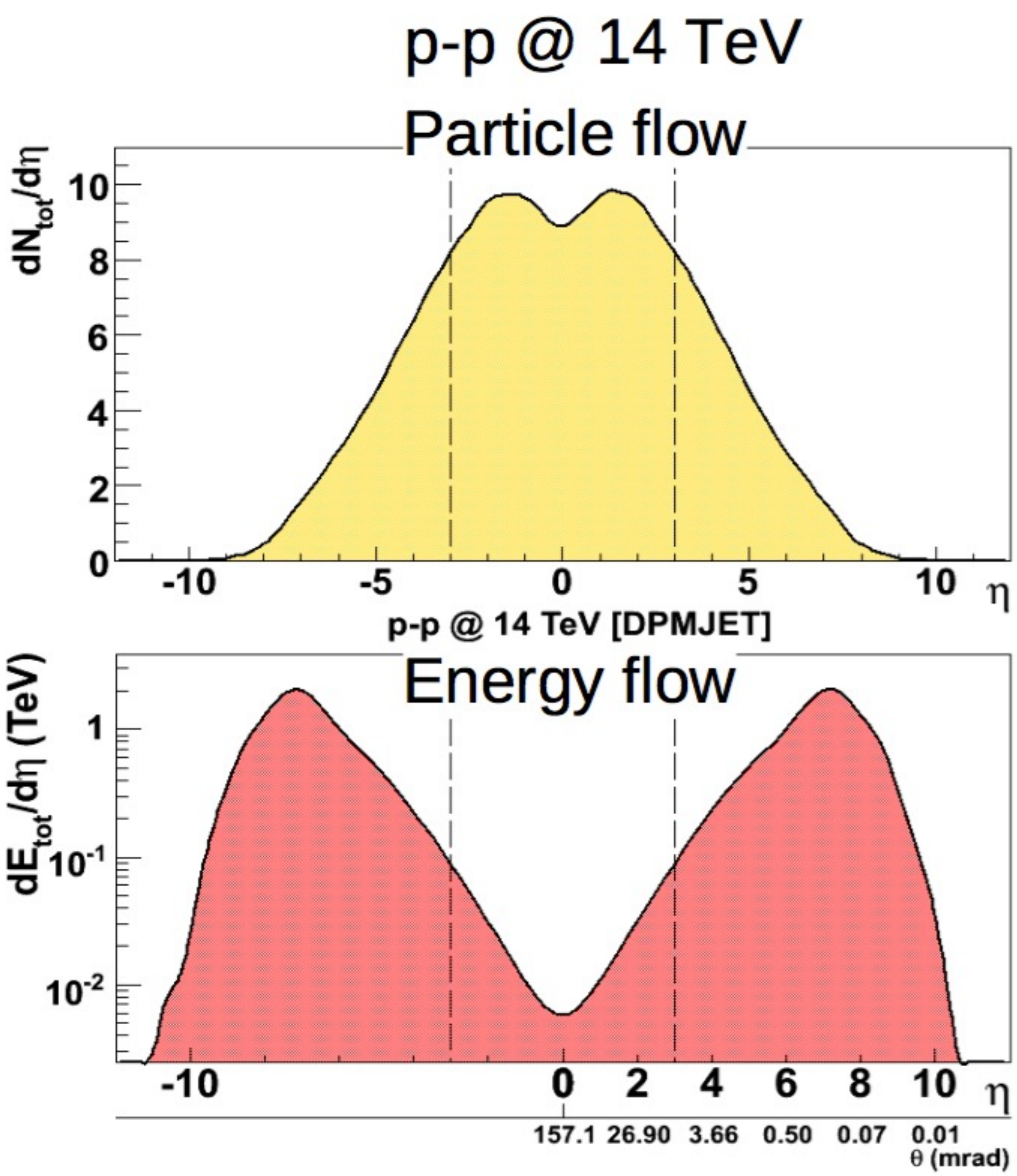

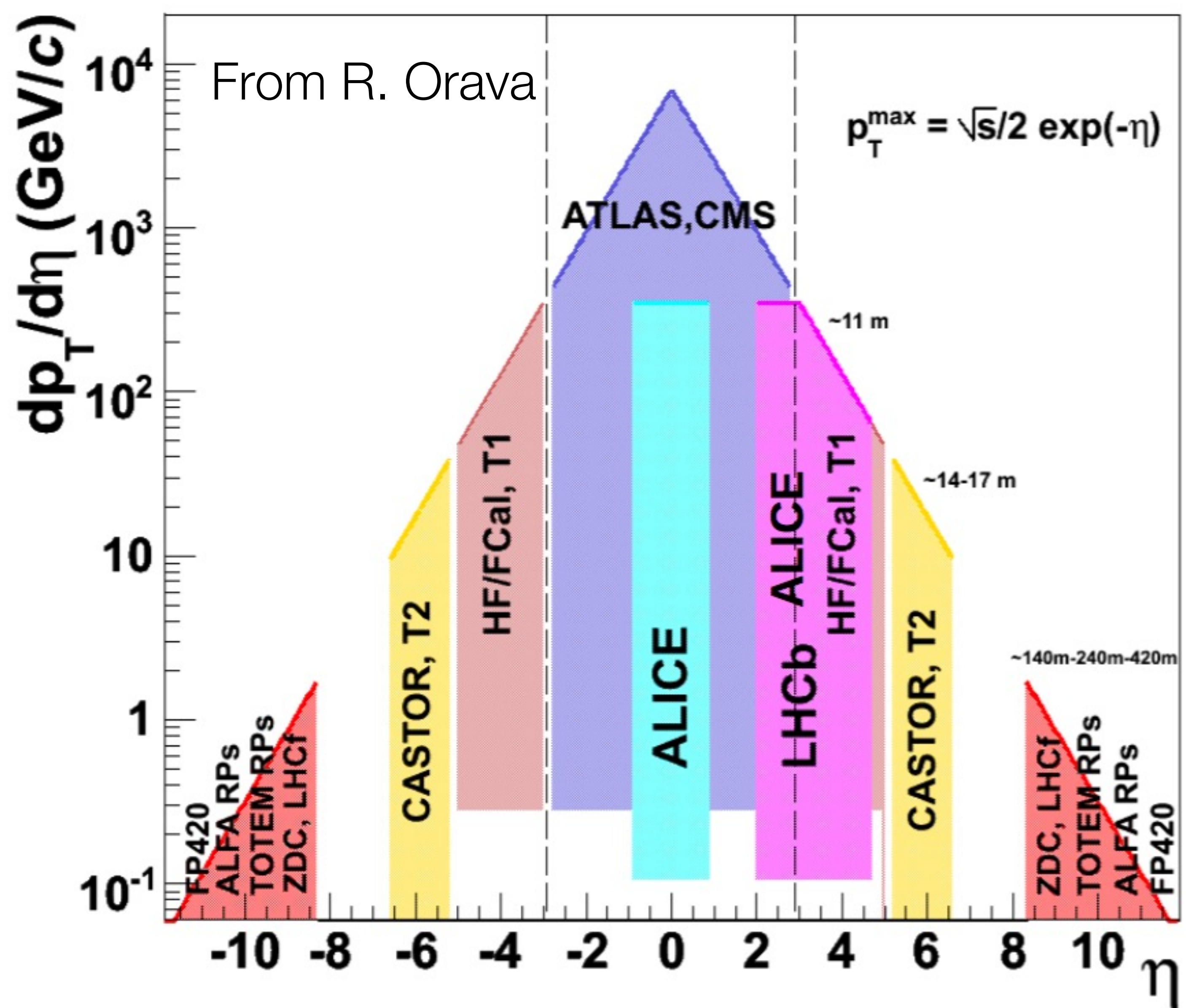

We may profit (and we are profiting) of the very broad coverage!

Dedicated forward detectors for a better measurement of the energy flow

LHCf, ZDC, TOTEM Roman Pots, ALFA, FP420

LHCf: how it is done and what it can measure

LHCf: location and detector layout

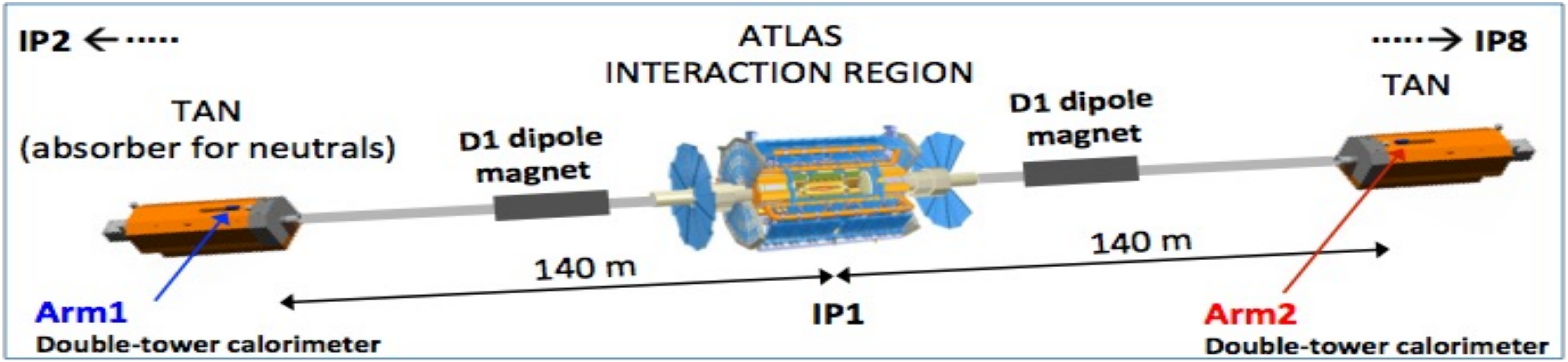

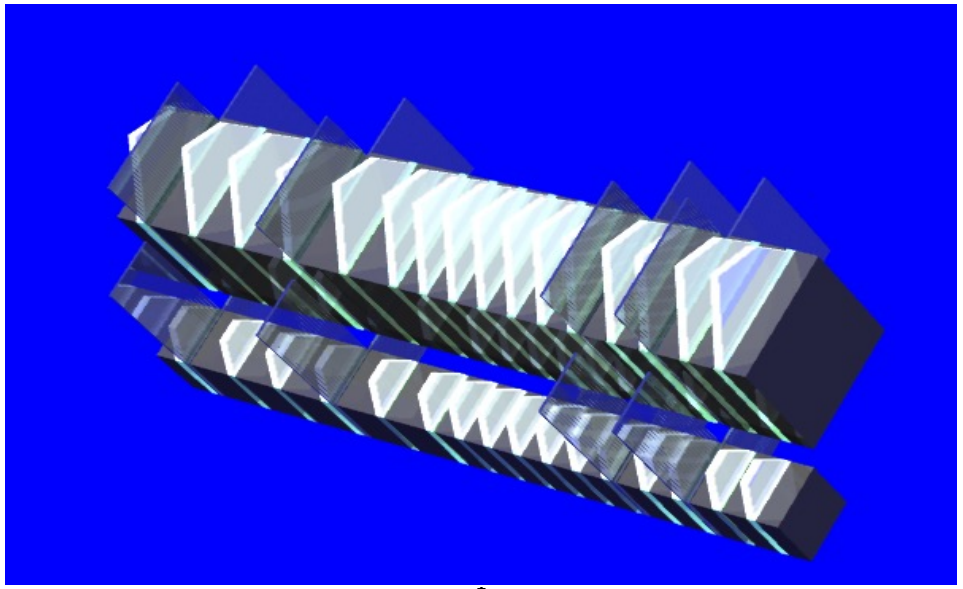

$44X_0$,
$1.6\ \lambda_{int}$

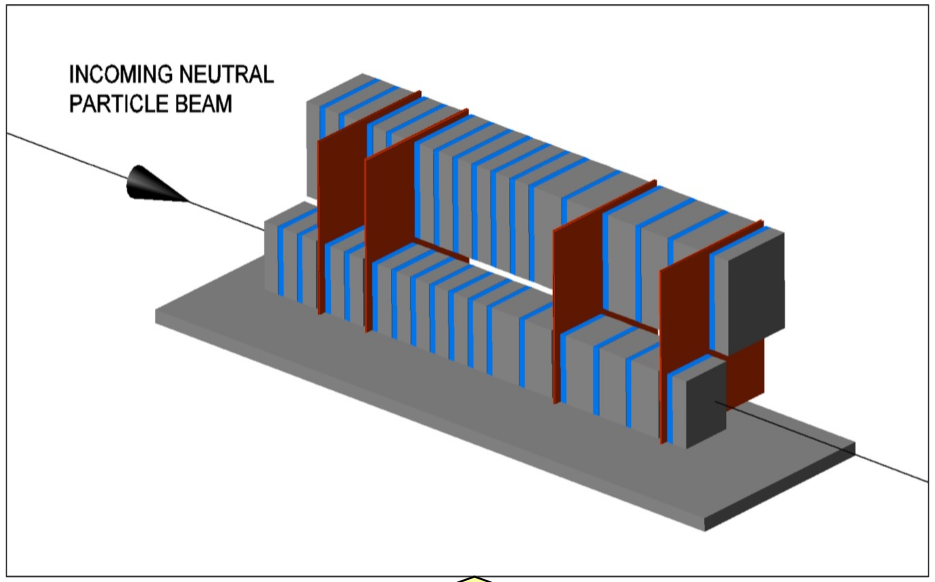

Arm#1 Detector
20mmx20mm+40mmx40mm
4 X-Y GSO Bars tracking layers

Energy resolution:
< 2% for photons
30% for neutrons
Position resolution:
< 200μm (Arm#1)
40μm (Arm#2)
Pseudo-rapidity range:
$\eta > 8.7$ @ zero Xing angle
$\eta > 8.4$ @ 140urad

Arm#2 Detector
25mmx25mm+32mmx32mm
4 X-Y Silicon strip tracking layers

Event category in LHCf: basic measurements

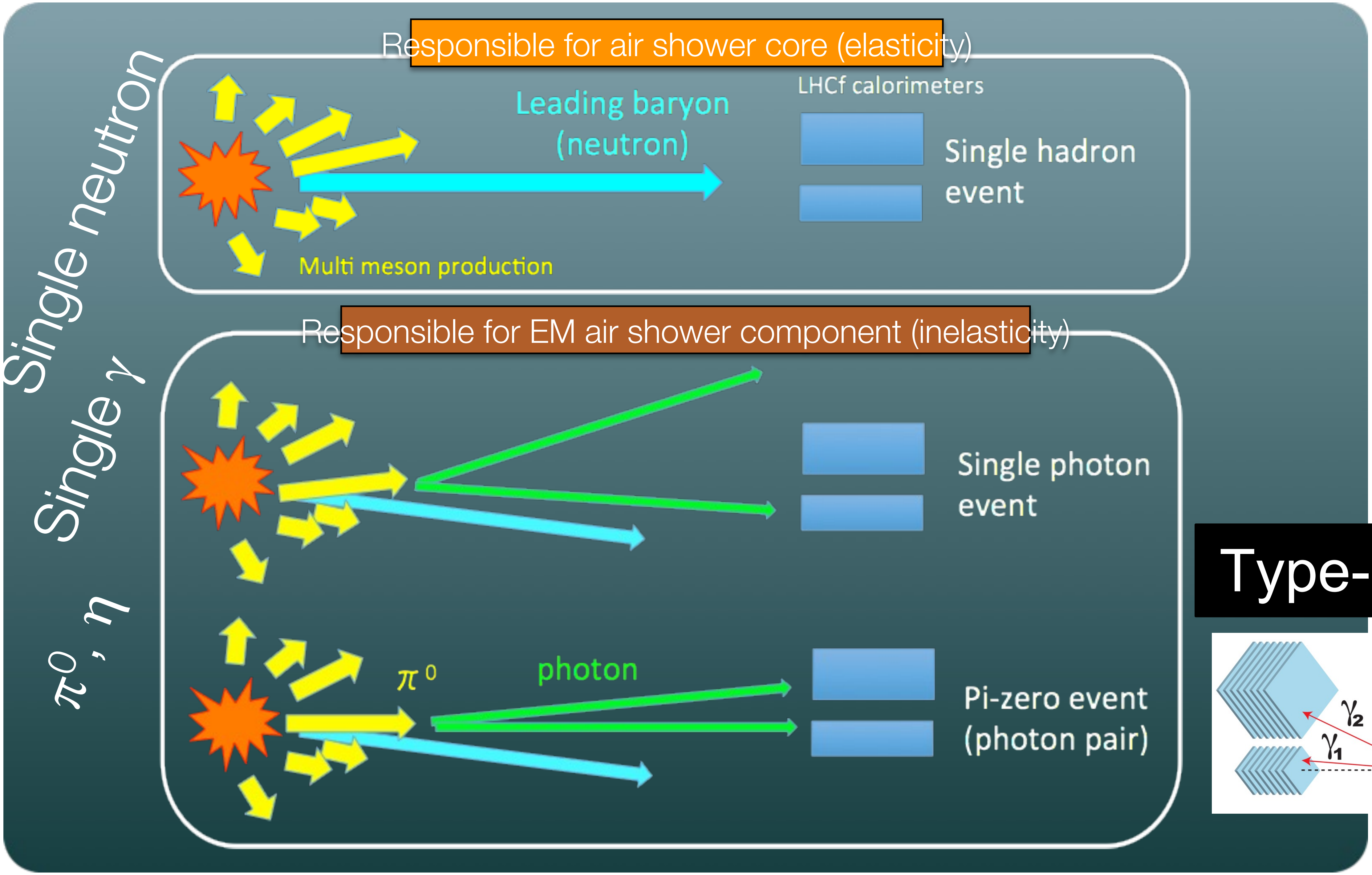

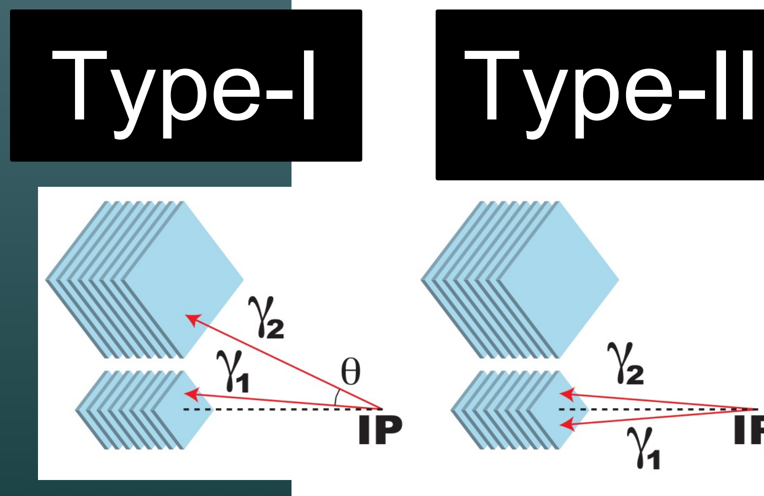

LHCf Data Taking and Analysis matrix

	γ	**neutron**	π^0	η^0
Detector Calibration	NIM A, 671, 129 (2012) JINST 12 P03023 (2017)	JINST 9 P03016 (2014)		
p+p 510 GeV (RHICf)	Submitted to PLB	Submitted to PRD	Phys. Rev. Lett. 124, 252501 (2021)	
p+p 900 GeV	Phys. Lett. B 715, 298 (2012)			
p+p 7 TeV	Phys. Lett. B 703, 128 (2011)	Phys. Lett. B 750 (2015) 360-366	Phys. Rev. D 86, 092001 (2012) Phys. Rev. D 94 032007 (2016)	
p+p 2.76 TeV			Phys. Rev. C 89, 065209 (2014) Phys. Rev. D 94 032007 (2016)	
p+Pb 5.02TeV				
p+p 13 TeV	PLB 780 (2018) 233-239	JHEP 11 (2018) 073 JHEP 07 (2020) 16	Analysis ongoing	JHEP 10 (2023) 169
p+Pb 8.1TeV	Analysis ongoing			
p+p 13 TeV	Analysis ongoing			

Main LHCf results

- We measure the neutral particle spectra
    - for different particles
        - n, γ, π^o, η
    - for different rapidity bins
    - eventually in different P_t/X_F (Feynman X) regions
- We compare our spectra with the 5 most commonly used high energy hadronic interaction models
    - EPOS-LHC
    - QGSJET II-04
    - DPMJET 3
    - SYBILL 2.3
    - PYTHIA 8

Neutron Production Cross Section
p-p $\sqrt{s}$ = 13 TeV

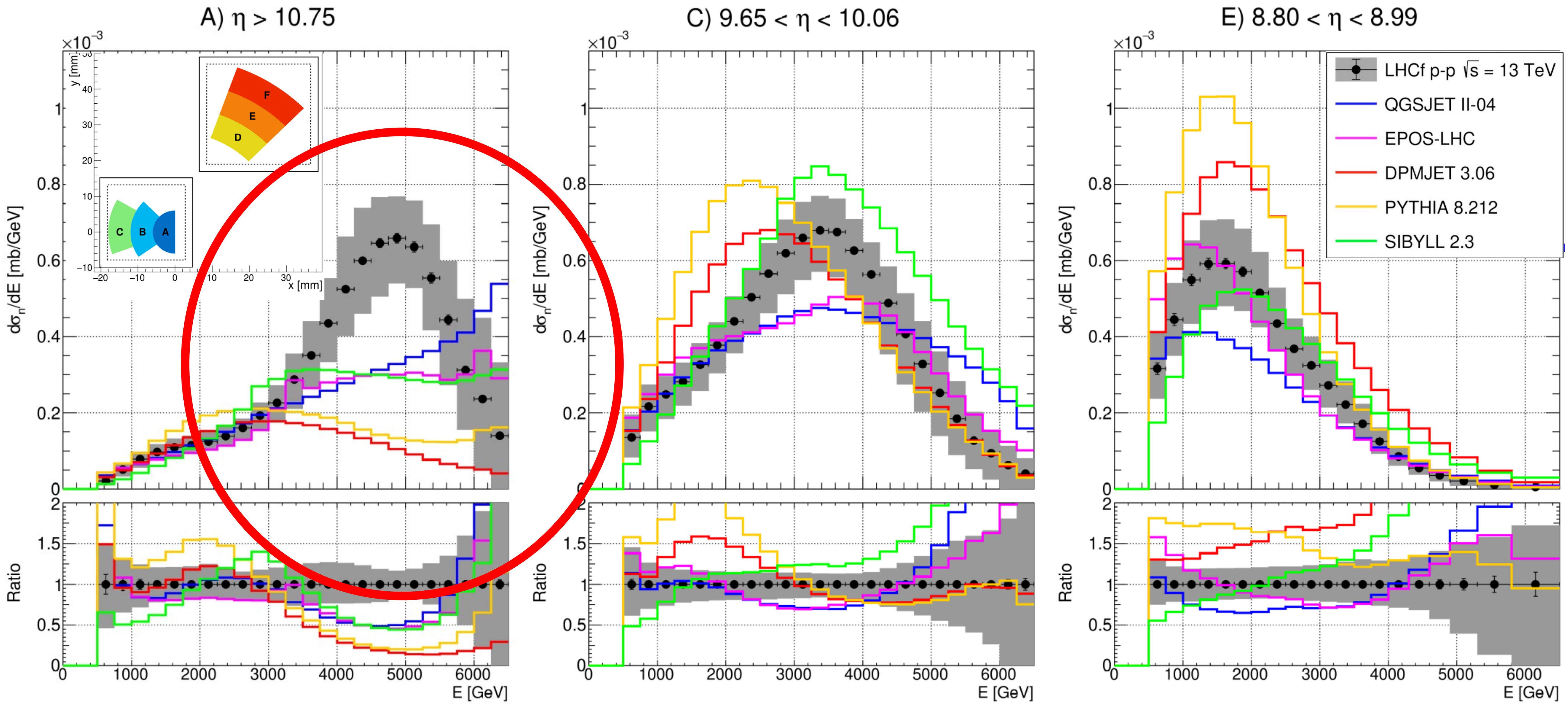

JHEP 07 (2020) 016

In η > 10.75 no model agrees with peak structure and production rate,
whereas in the other regions, **SIBYLL 2.3** and **EPOS-LHC** have better but not satisfactory agreement with the experimental measurements*

Neutron Energy Flow & Inelasticity

p-p $\sqrt{s}$ = 13 TeV

$dE_n/d\eta$

Energy Flow

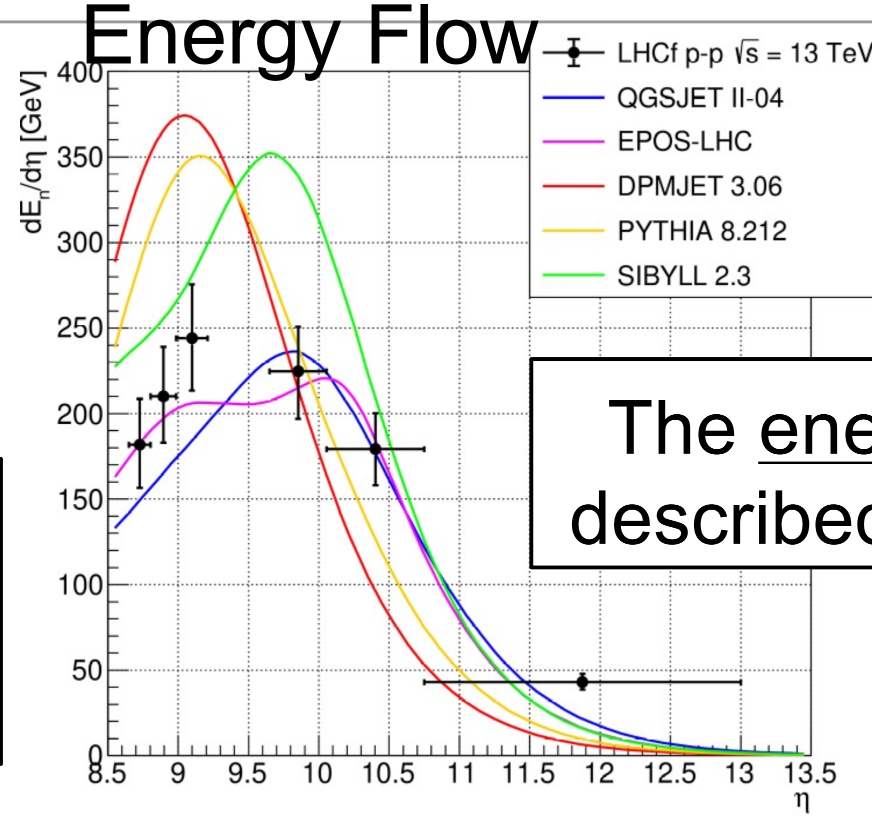

The energy flow is well described by **EPOS-LHC**

Most models reproduce the average inelasticity but not the distribution

$$k = 2E/\sqrt{s}$$

Elasticity

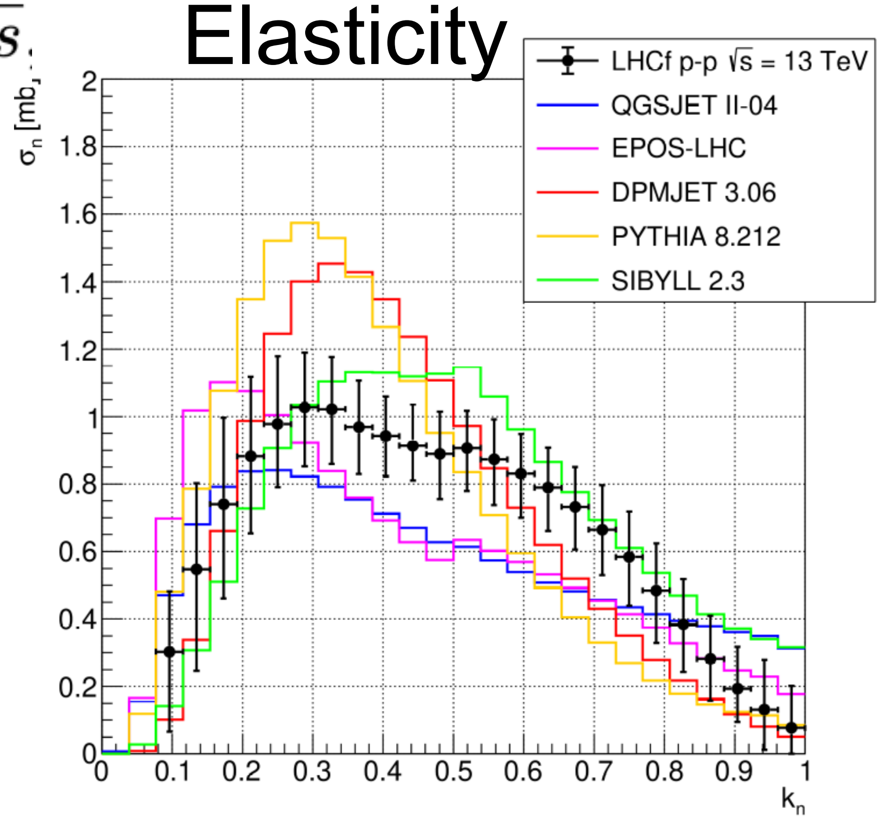

<Inelasticity>

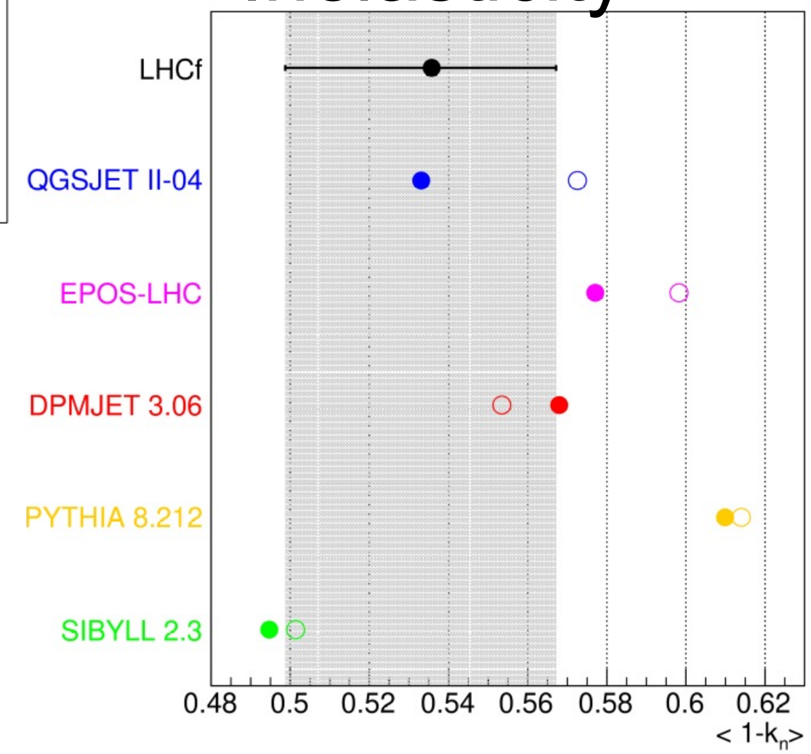

JHEP 07 (2020) 016

Photons dσ/dE

p-p $\sqrt{s}$ = 13 TeV

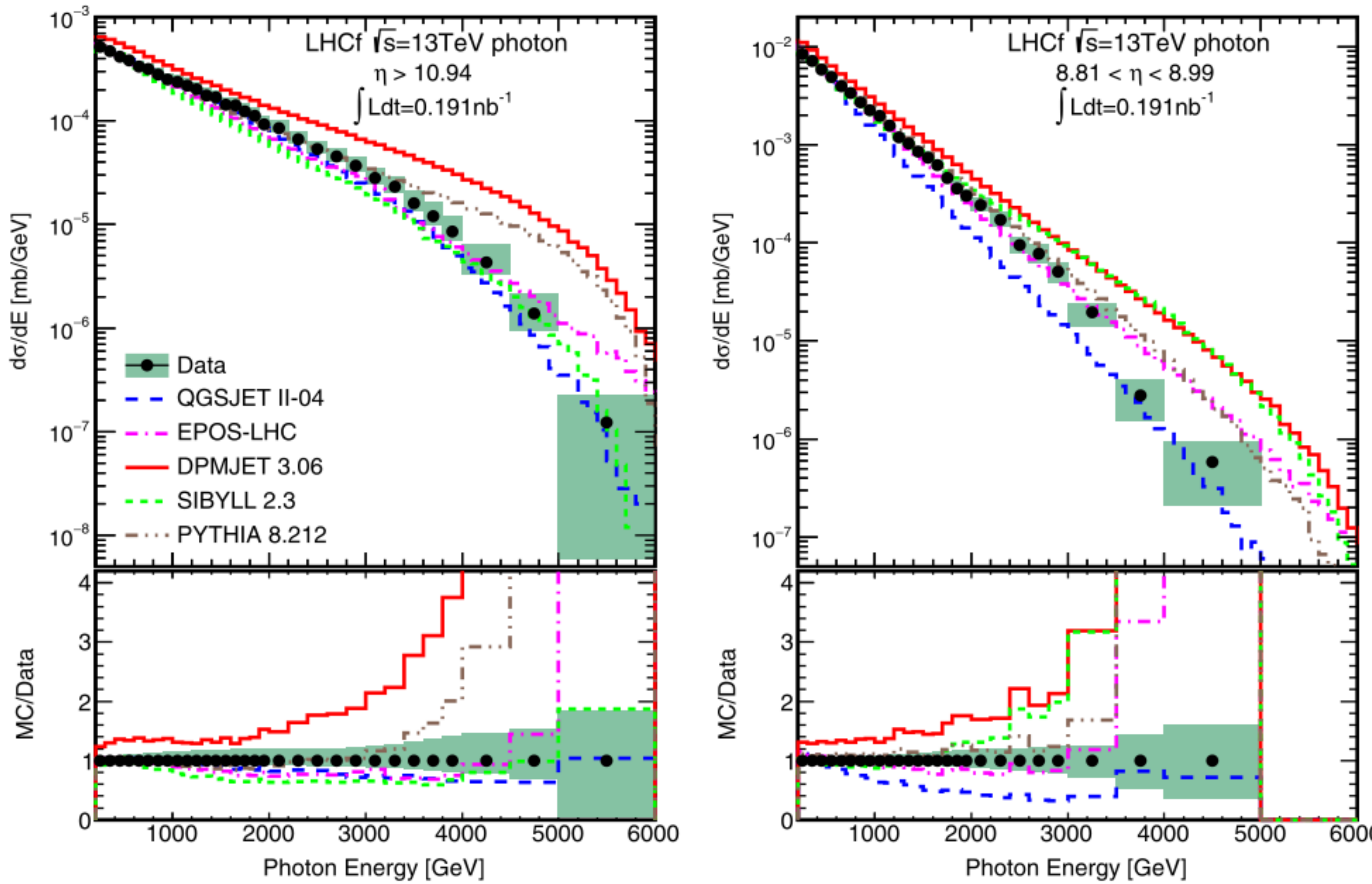

PLB 780 (2018) 233-239

QGSJET II-04 is in good agreement for η>10.94, otherwise softer

EPOS-LHC is in good agreement below 3-5 TeV, otherwise harder

Test of Feynman scaling
using forward photons

Using γ in $\sqrt{s}$=510 GeV (RHICf) and 7 or 13 TeV (LHCf)

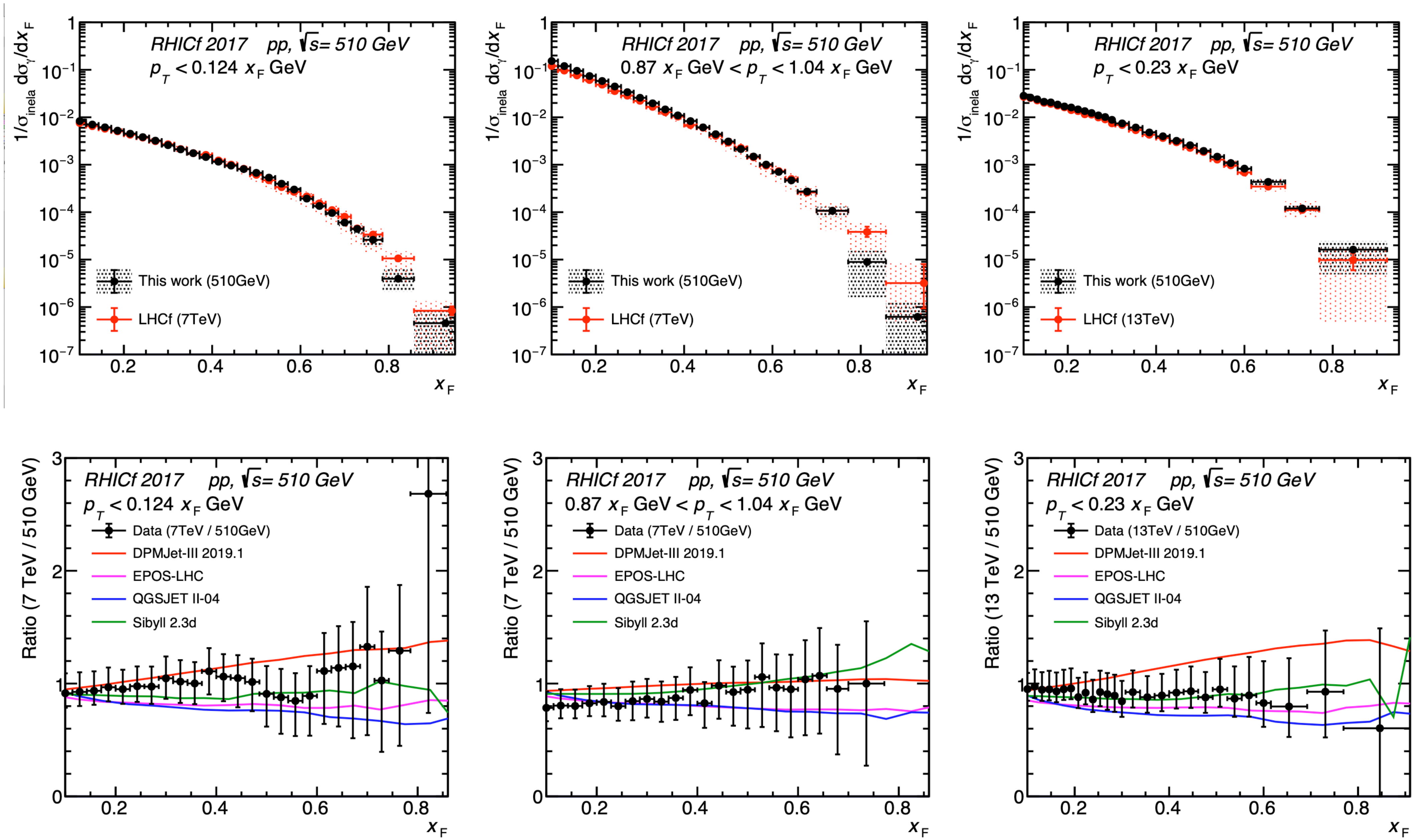

ArXiv:2203.15416
...submitted to PLB

First confirmation of **Feynman scaling** using zero-degree photons
but no sensitivity to small x_F dependency as in some models

η Production Rate

p-p $\sqrt{s}$ = 13 TeV

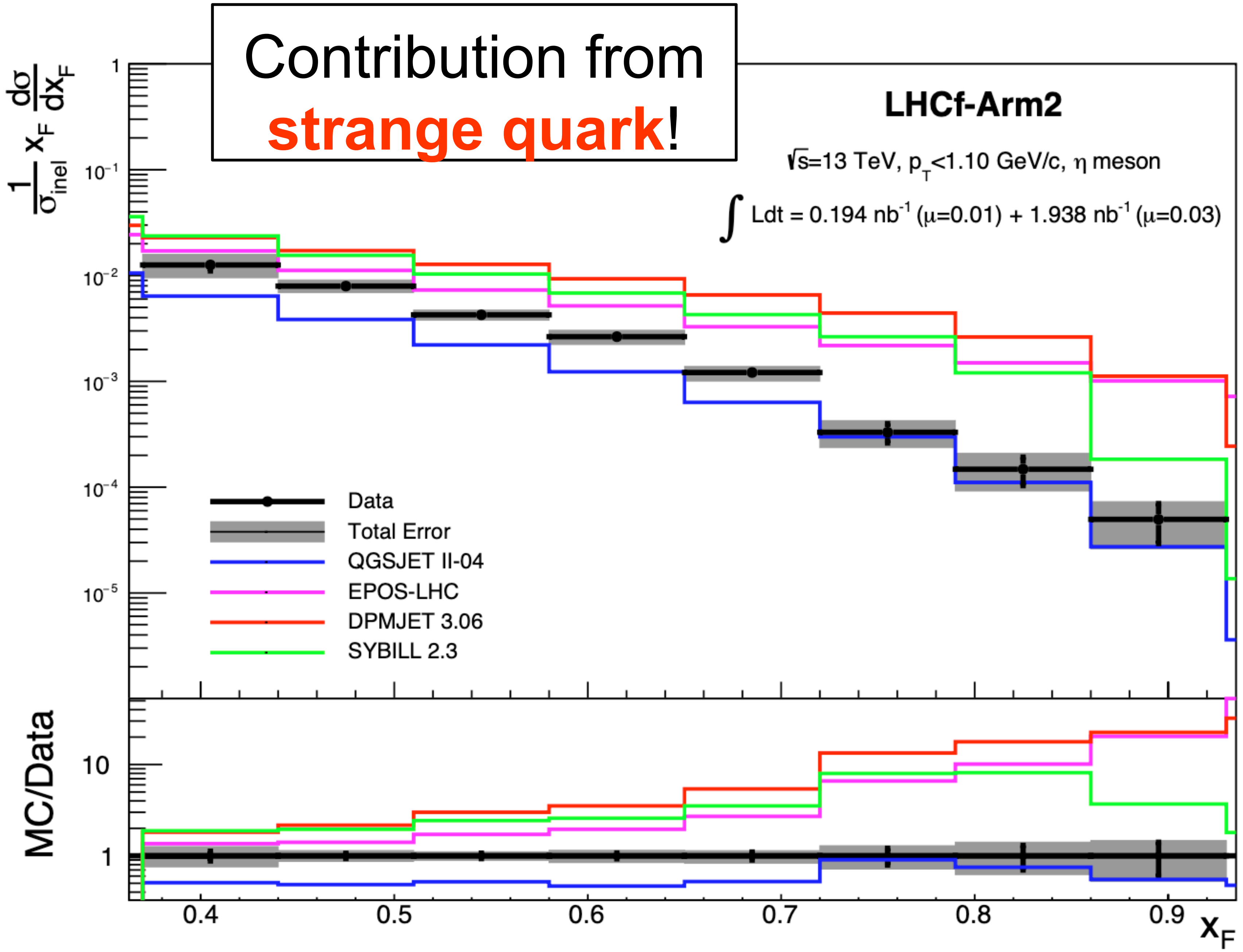

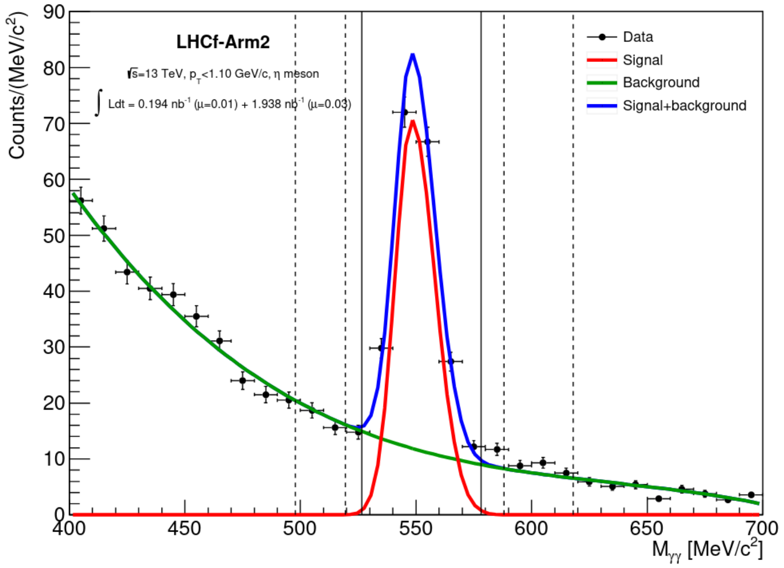

ArXiv:2305.06633
CERN-EP-2023-076
JHEP 10 (2023) 169

Among the large model variations, only **QGSJETII-04** has good but not satisfactorily agreement with the experimental measurements

LHCf in Run III: p-O

Foreseen in 2024

Main Motivation

Both p-p and p-Pb collisions are not representative of the first interaction of a UHECR (which is a light nucleus) with an atmospheric nucleus (mainly N or O), hence *the importance of p-O (and O-O) operations to avoid large extrapolation*

In addition, the main uncertainty in forward production from p-Pb collisions is due to contribution from Ultra-Peripheral Collisions (UPC background), which is irrelevant in the EAS case

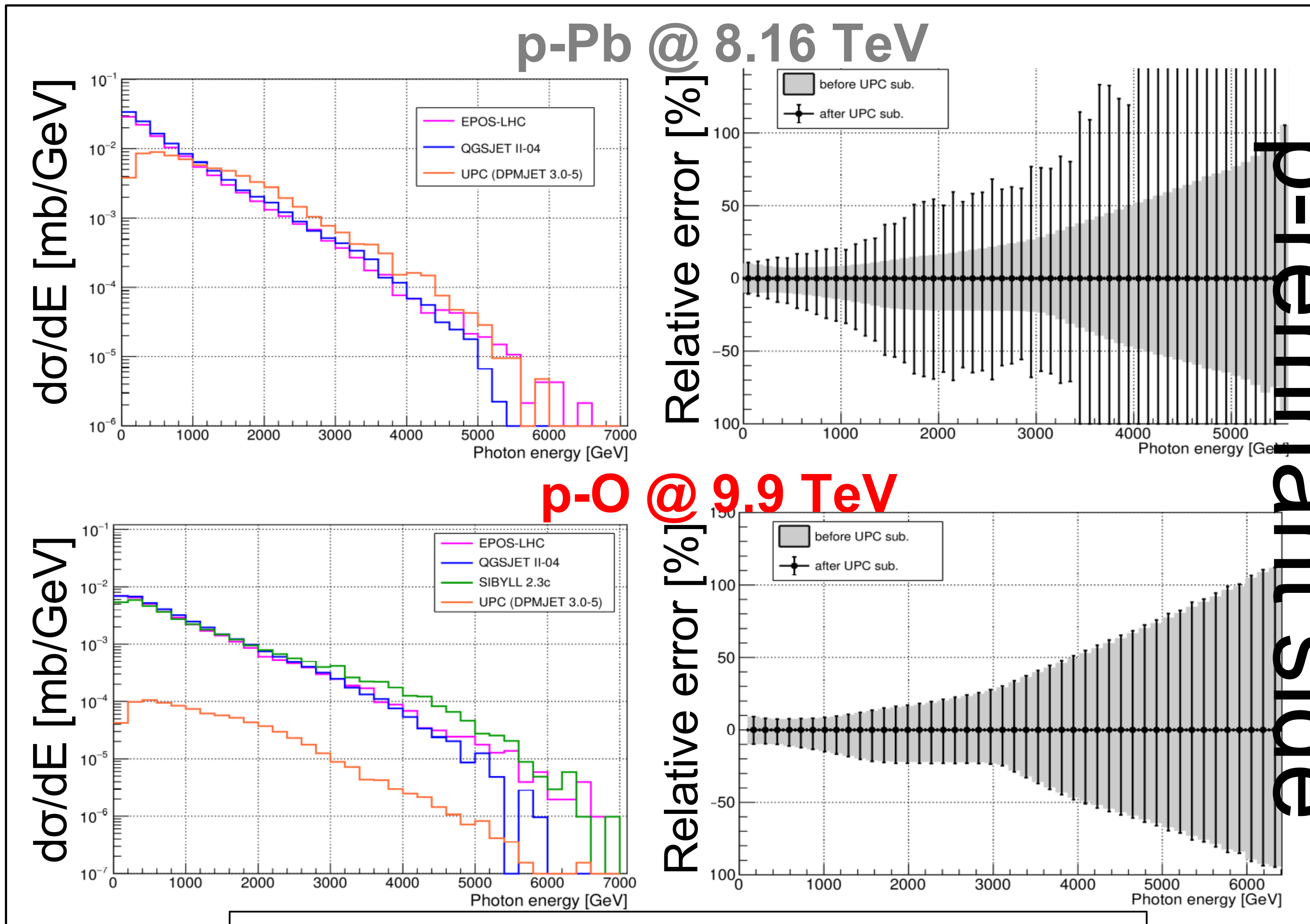

Forward photon production in η > 10.94

Run III is the **last opportunity** for LHCf!

A **week** of p-O (and possibly O-O) operations foreseen for **2024**

Combining forward and central info (ATLAS highlight)

- In p+p collisions
  - Forward spectra of Diffractive/ Non-diffractive events
  - Forward hadron vs central activity correlation
  - Measurement of proton-π collisions
  - Forward measurements vs very forward protons in AFP and RP

All are important for precise-understanding of CR air shower development

- Sharing of LHCf trigger with ATLAS
  - Operation in 2013
    - p+Pb, $\sqrt{s_{NN}} = 5$TeV

    → about 10 M common events.
  - Operation in 2015
    - p+p, $\sqrt{s} = 13$TeV

    → about 6 M common events.
  - Operation in 2016
    - p+Pb, $\sqrt{s_{NN}} = 5$TeV

    → about 26 M common events
    - p+Pb, $\sqrt{s_{NN}} = 8$TeV

    → about 16 M common events
  - Operation in 2023
    - p+p, $\sqrt{s} = 13.6$TeV

    → about 240 M common events

LHCf-"ATLAS central" joint analysis

Preliminary result for photons in p-p $\sqrt{s}$ = 13 TeV

After a preliminary test in 2013,
in 2015 and 2016 LHCf and ATLAS
experiments had **common operation**.

Diffractive events can be distinguished
from non-diffractive events
by **ATLAS veto** : tracks=0 at |η|<2.5

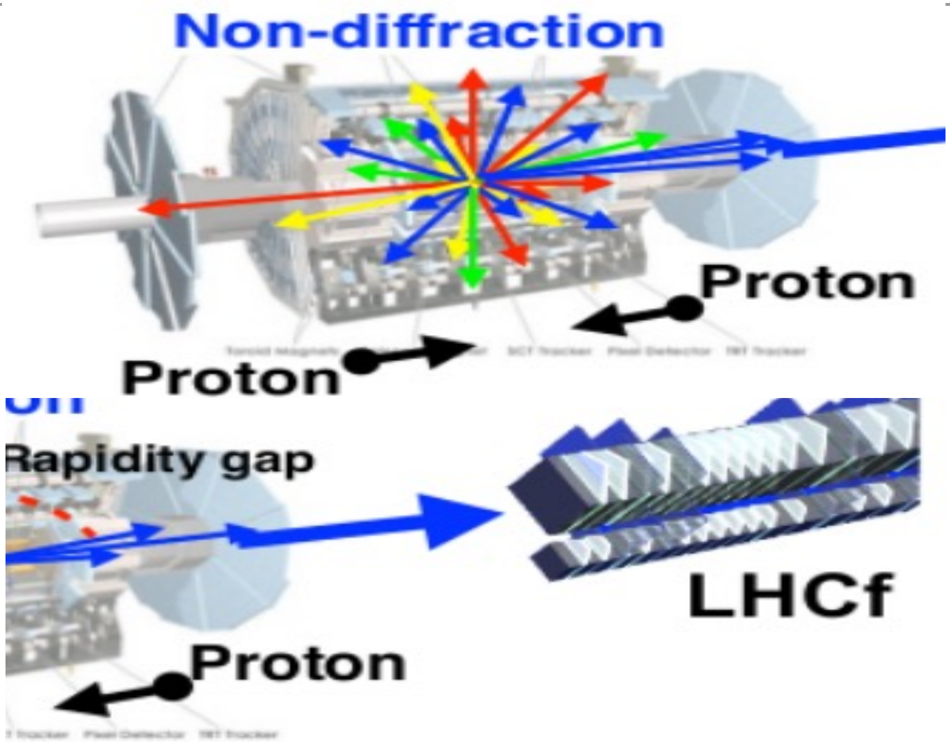

$N_{veto}/N_{inclusive}$

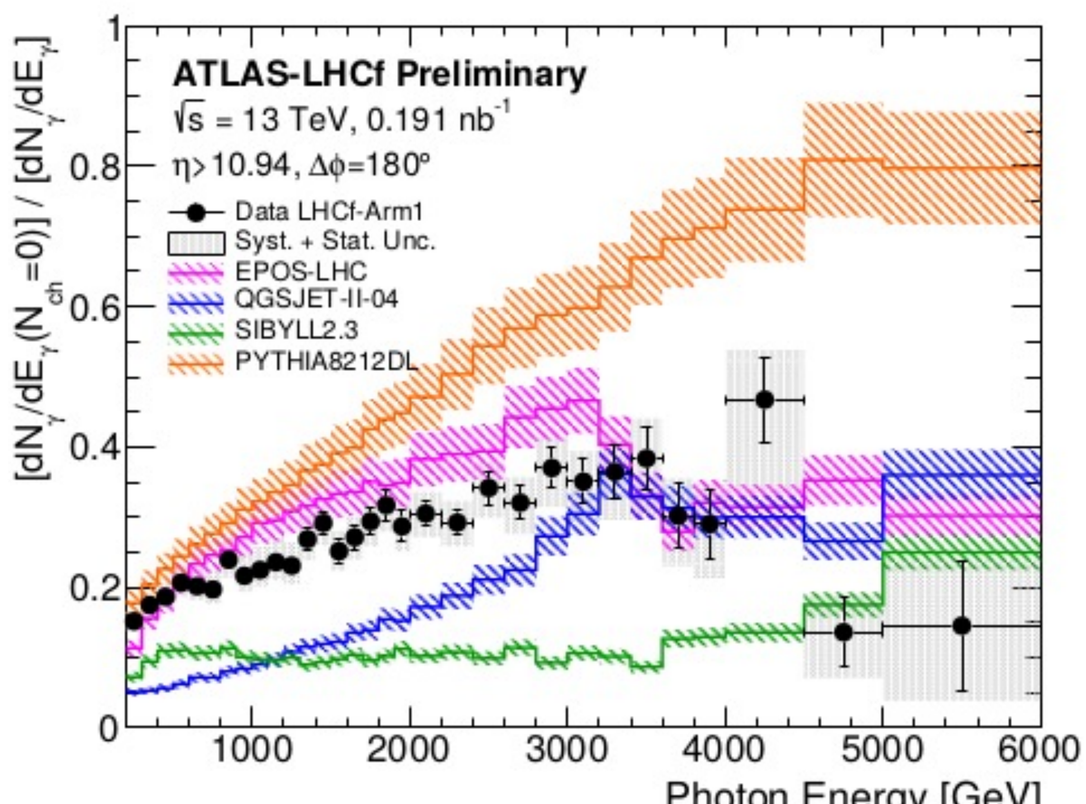

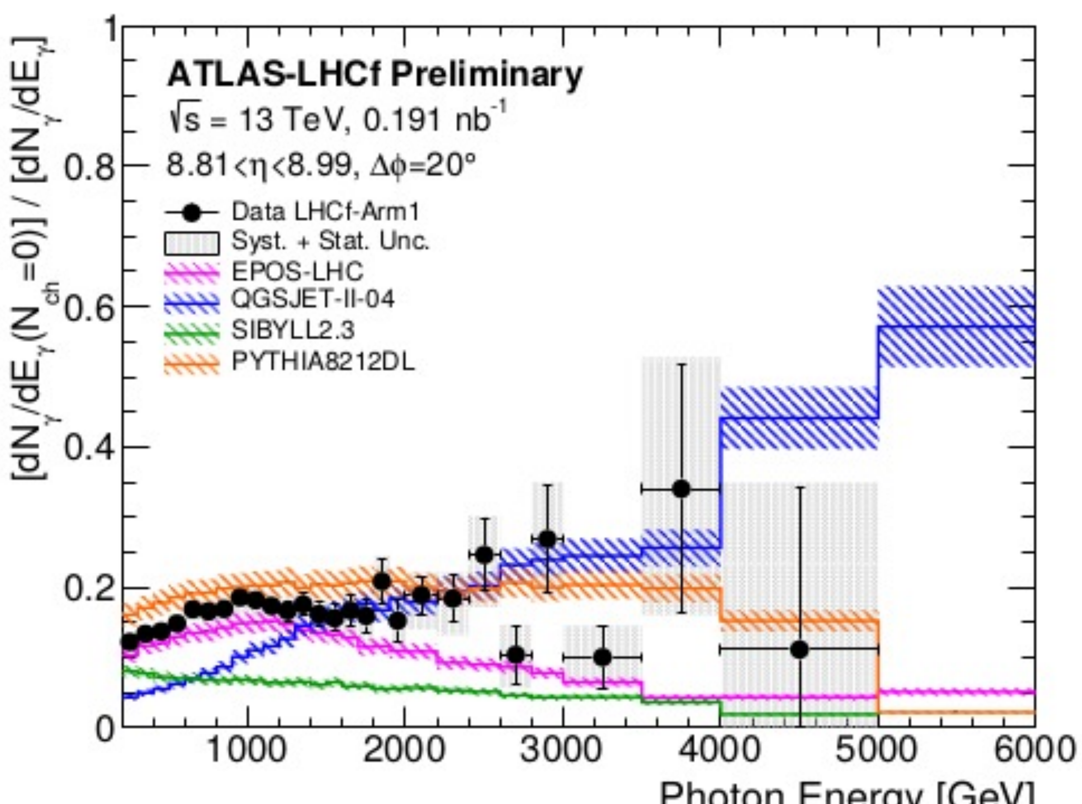

ATLAS-CONF-2017-075

…paper in finalization

Operations with ATLAS ZDC

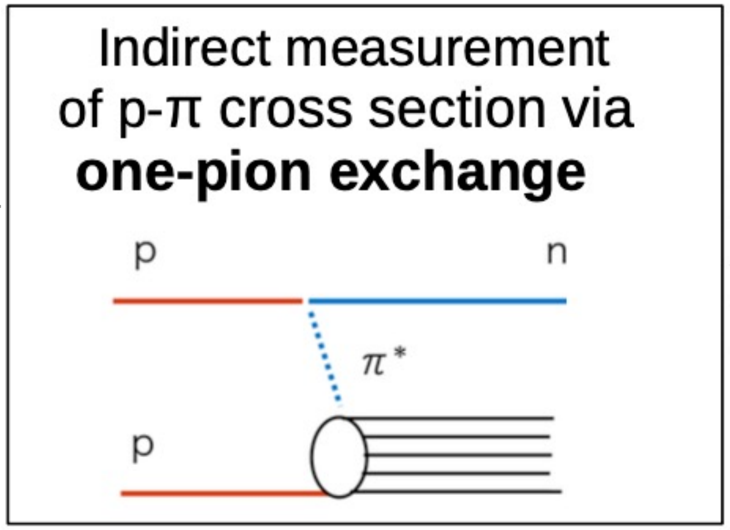

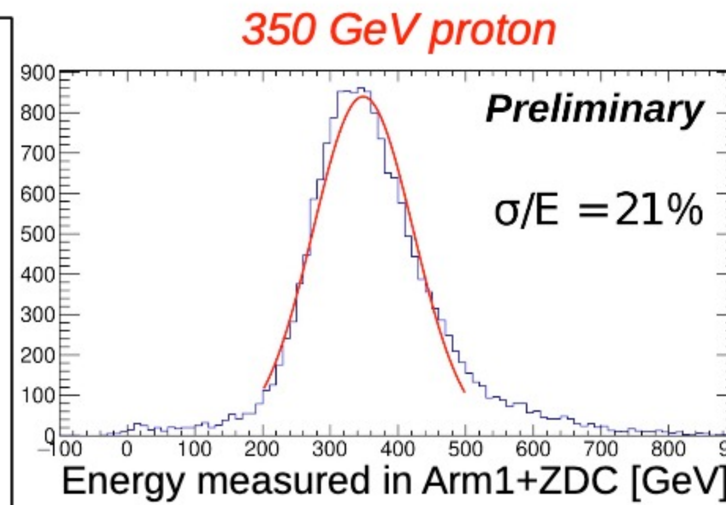

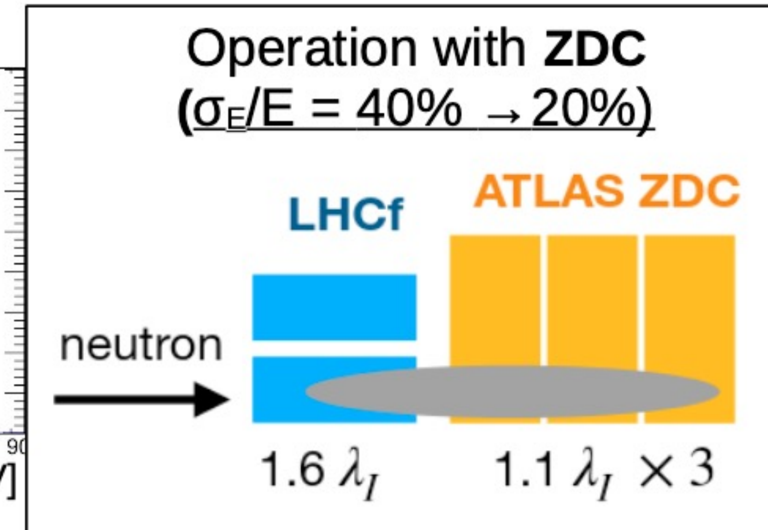

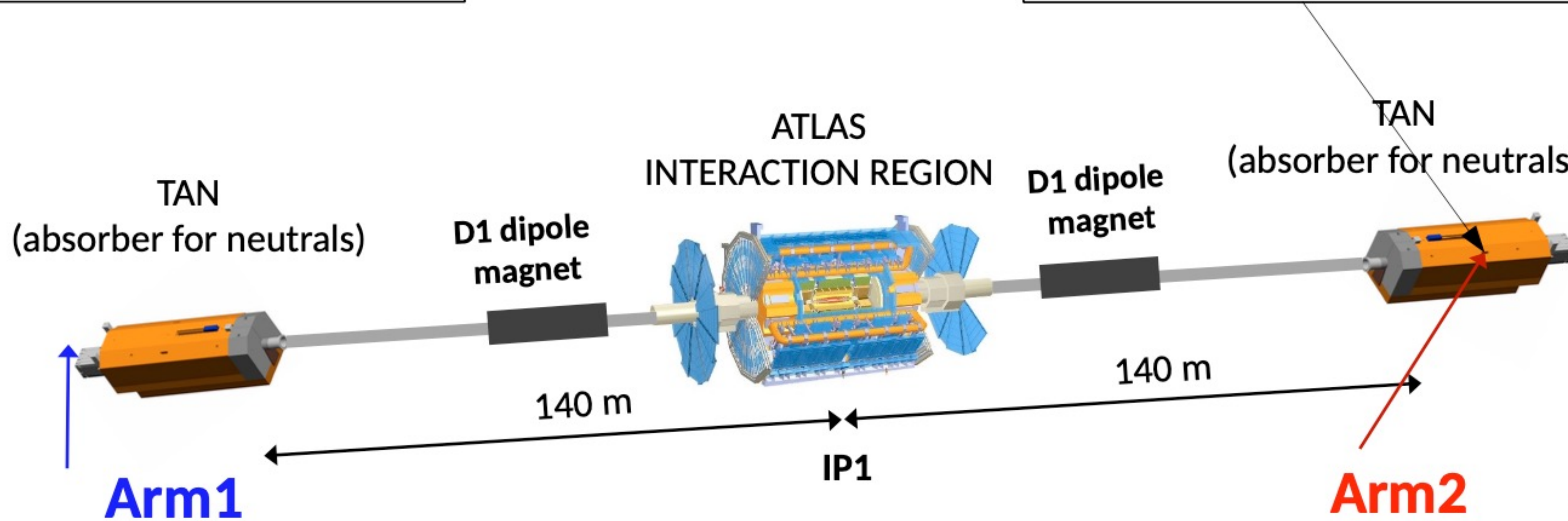

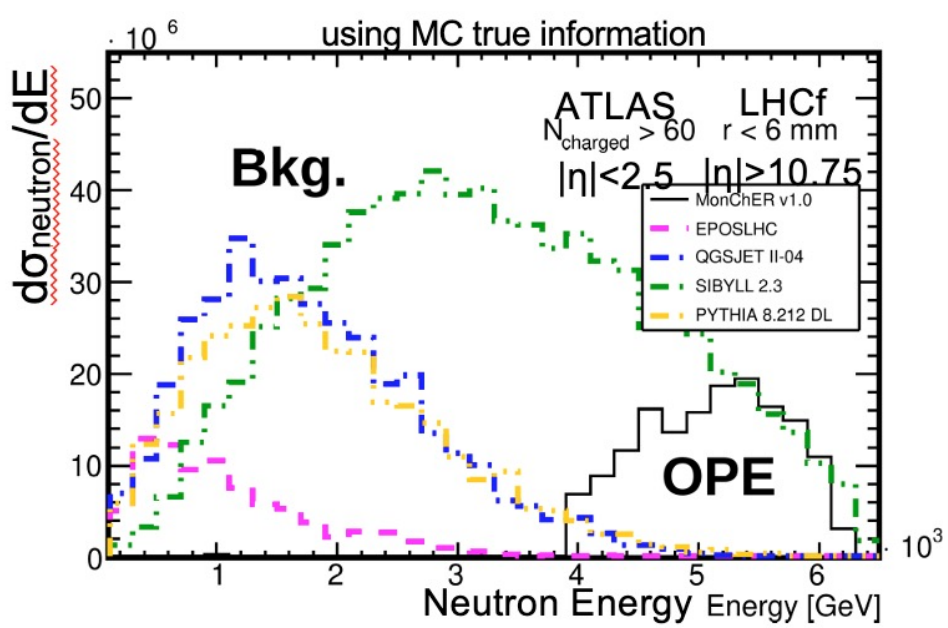

Main point:
improvement of the neutron energy resolution

Operations with ATLAS AFP

ATLAS PUB Note
ANA-STDM-2022-13
22nd August 2023

Physics potential of a combined data taking of the LHCf and ATLAS Roman Pot detectors

Identification of **single diffractive events**
+ possible measurements of:
- *Δ resonance* ($p+p \rightarrow p+\Delta \rightarrow p+p+\pi^0$)
- Bremsstrahlung ($p+p \rightarrow p+p+\gamma$)

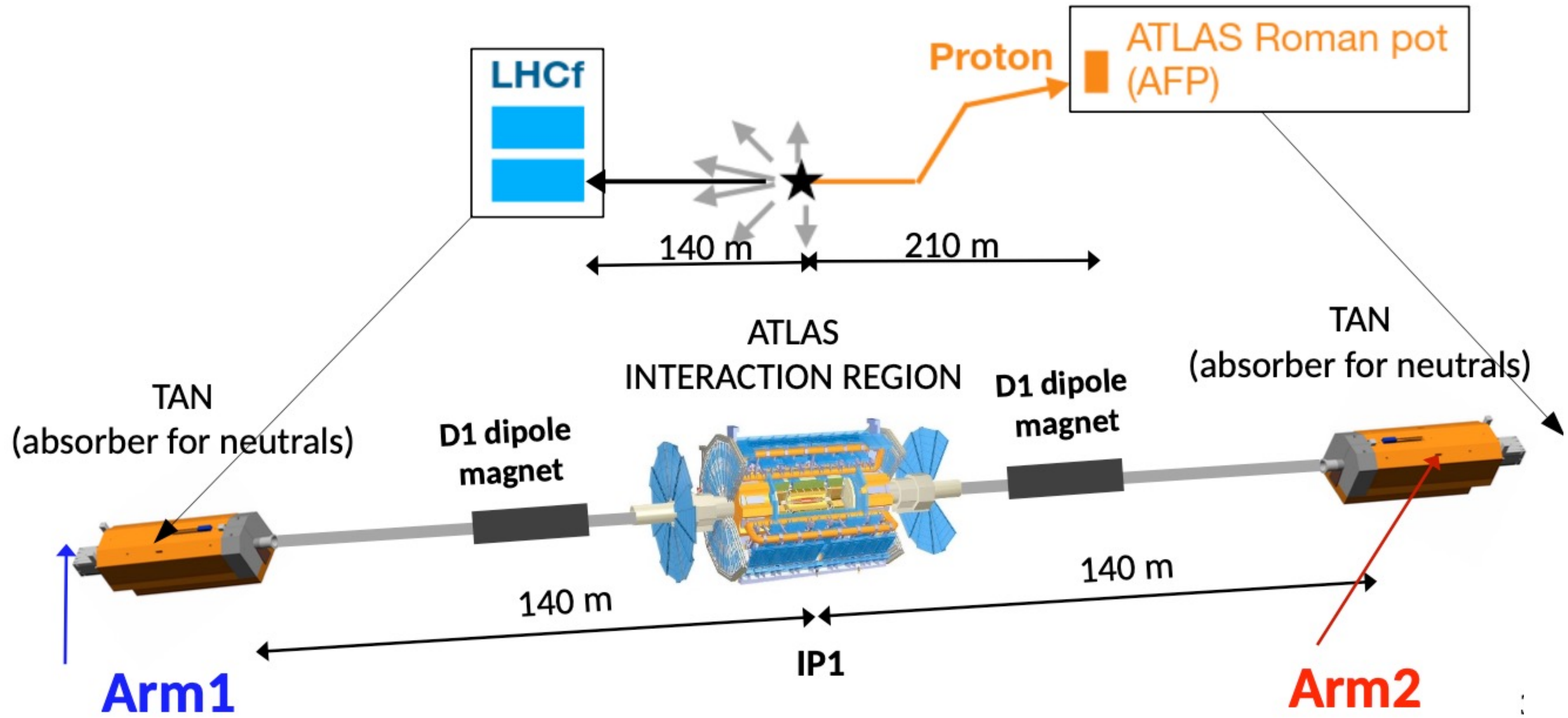

AFP: 205 m and 217 m
ALFA: 237 m and 245 m

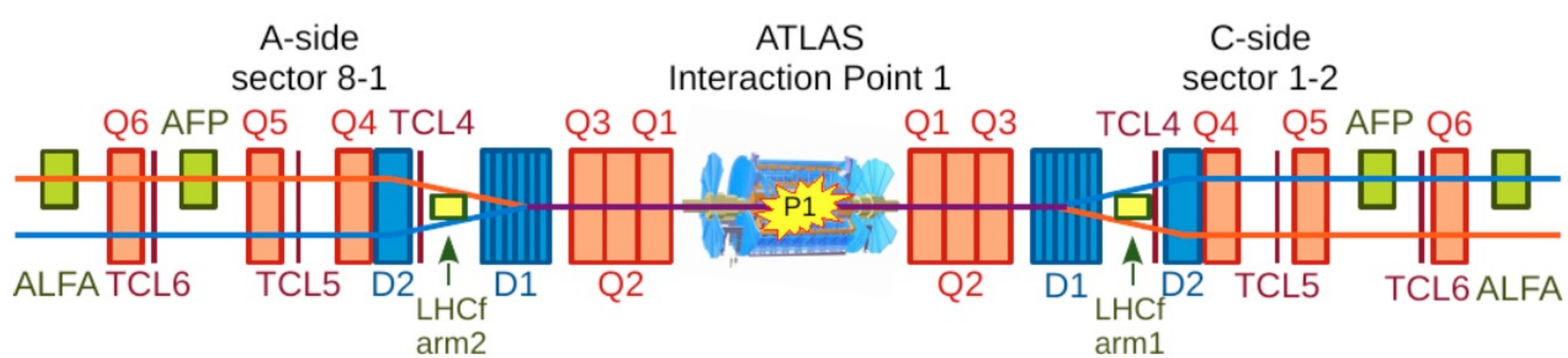

AFP+LHCf | ALFA+LHCf

Single Diffr.

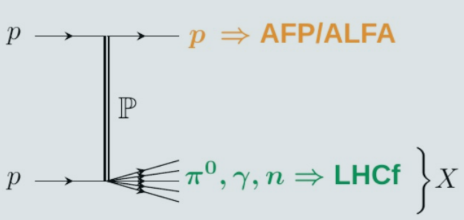

(a) Single diffraction

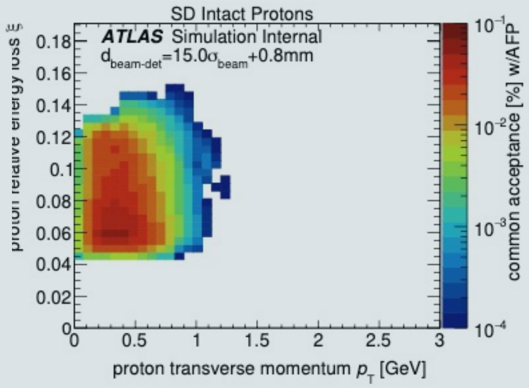

(a) Single diffraction (AFP near station)

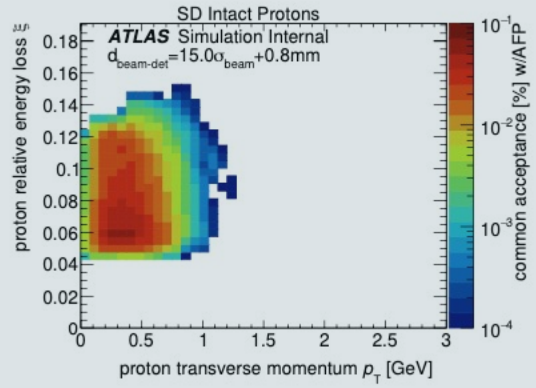

(b) Single diffraction (AFP far station)

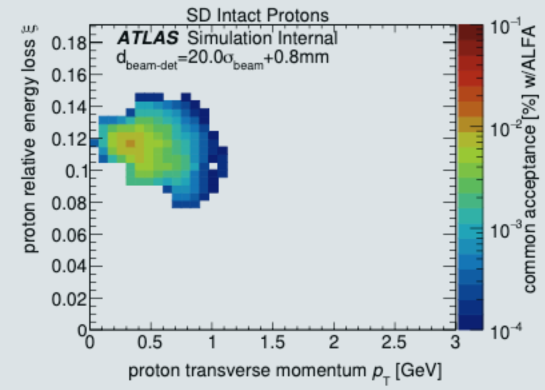

(a) Single diffraction (ALFA near station)

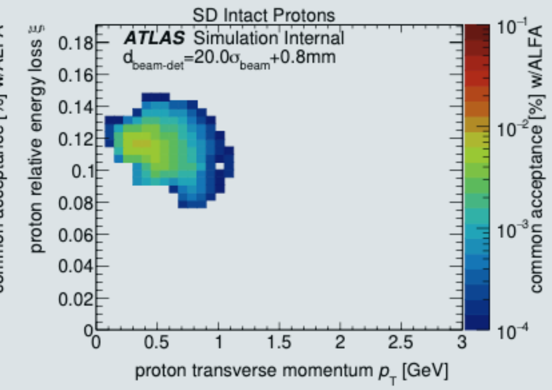

(b) Single diffraction (ALFA far station)

$\Delta^+(1232)$

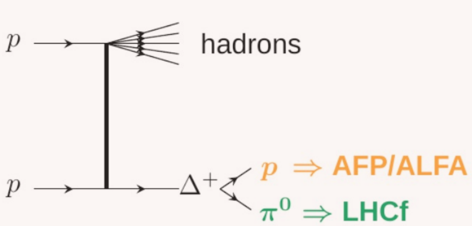

(b) $\Delta^+(1232)$ excitation

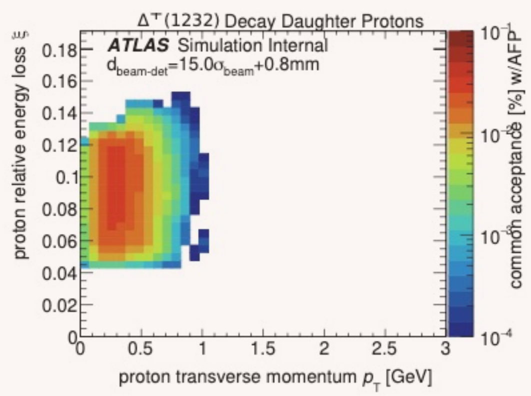

(c) $\Delta^+(1232)$ production (AFP near station)

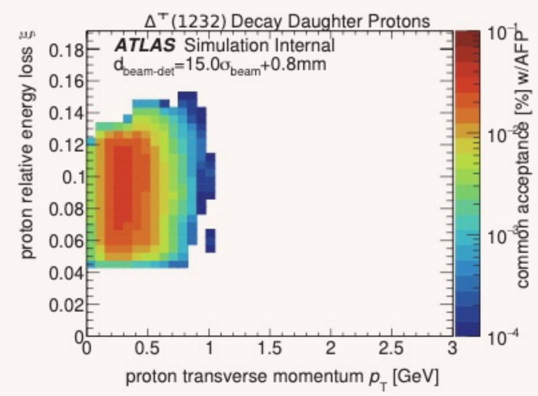

(d) $\Delta^+(1232)$ production (AFP far station)

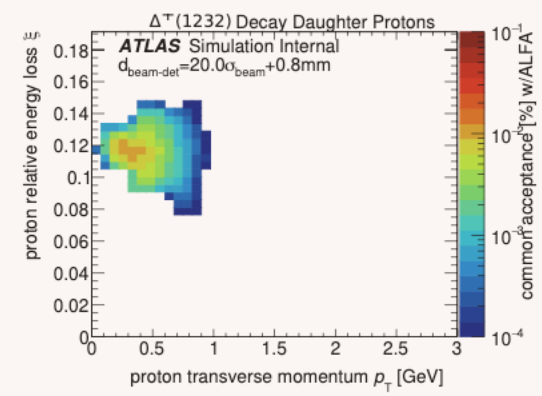

(c) $\Delta^+(1232)$ production (ALFA near station)

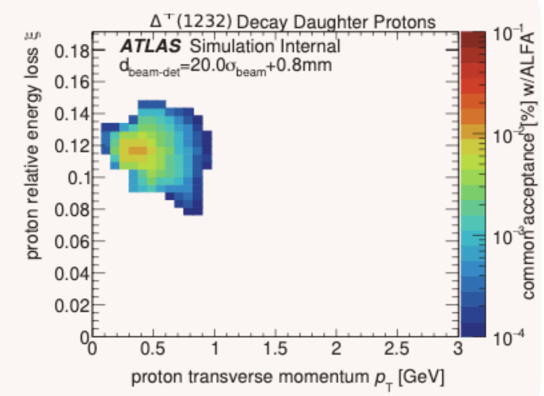

(d) $\Delta^+(1232)$ production (ALFA far station)

N(1440)

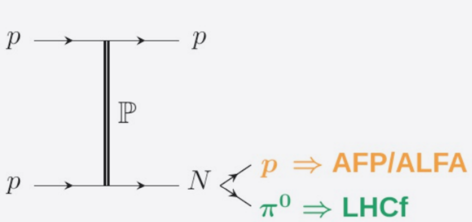

(c) $N(1440)$ excitation

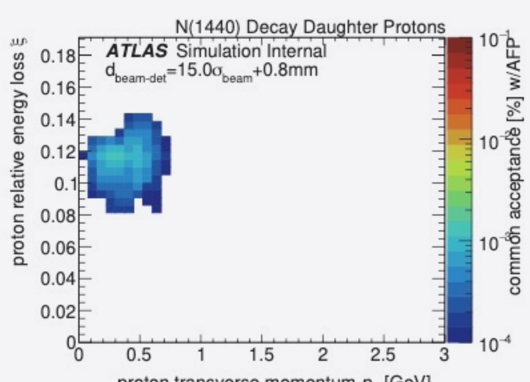

(e) $N(1440)$ production (AFP near station)

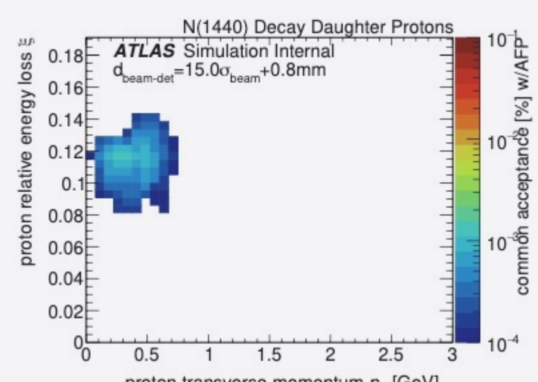

(f) $N(1440)$ production (AFP far station)

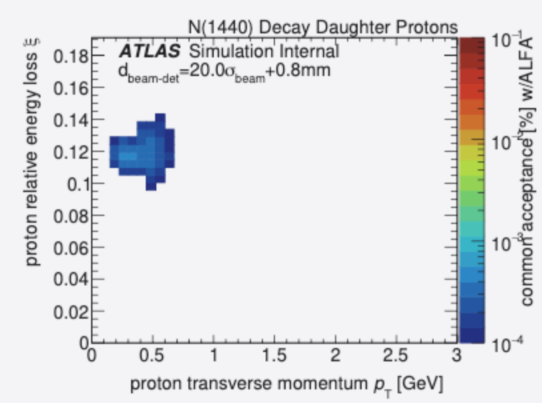

(e) $N(1440)$ production (ALFA near station)

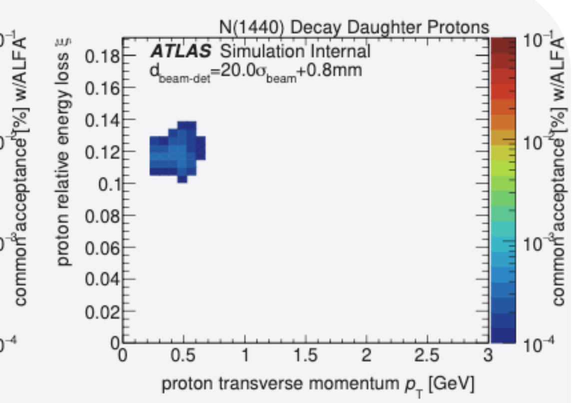

(f) $N(1440)$ production (ALFA far station)

Figure 18: Combined acceptance maps for the studied processes with AFP near and far stations, respectively.

Figure 19: Combined acceptance maps for the studied processes with ALFA near and far stations, respectively.

A recent highlight from CMS: Nonresonant central exclusive production of charged hadron pairs

Available on the CERN CDS information server

CMS PAS SMP-21-004
TOTEM NOTE 2023-001

CMS Physics Analysis Summary

Contact: cms-pag-conveners-smp@cern.ch

2023/08/15

Nonresonant central exclusive production of charged hadron pairs in proton-proton collisions at $\sqrt{s} = 13$ TeV

The CMS and TOTEM Collaborations

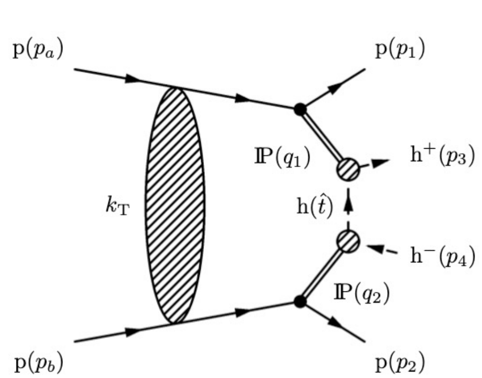

Figure 2: Feynman diagram for the nonresonant continuum of central exclusive production of hadron pairs via double pomeron exchange, including the rescattering correction.

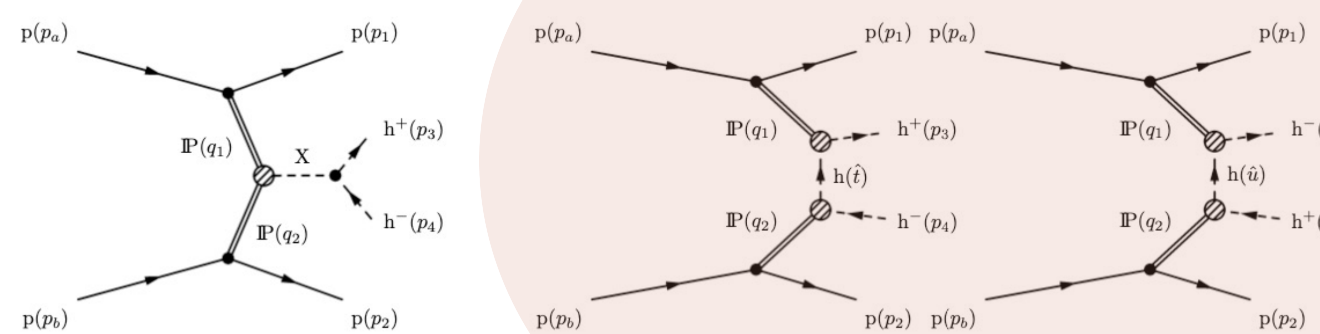

Figure 1: Born-level Feynman diagrams for central exclusive production of hadron pairs via double pomeron exchange, depicting resonant (left) and nonresonant continuum (rightmost two) contributions.

Differential cross sections measured in many different phase space regions

$d^3\sigma/dp_{1,T}dp_{2,T}d\phi$ as a function of ϕ in several $(p_{1,T}, p_{2,T})$ bins

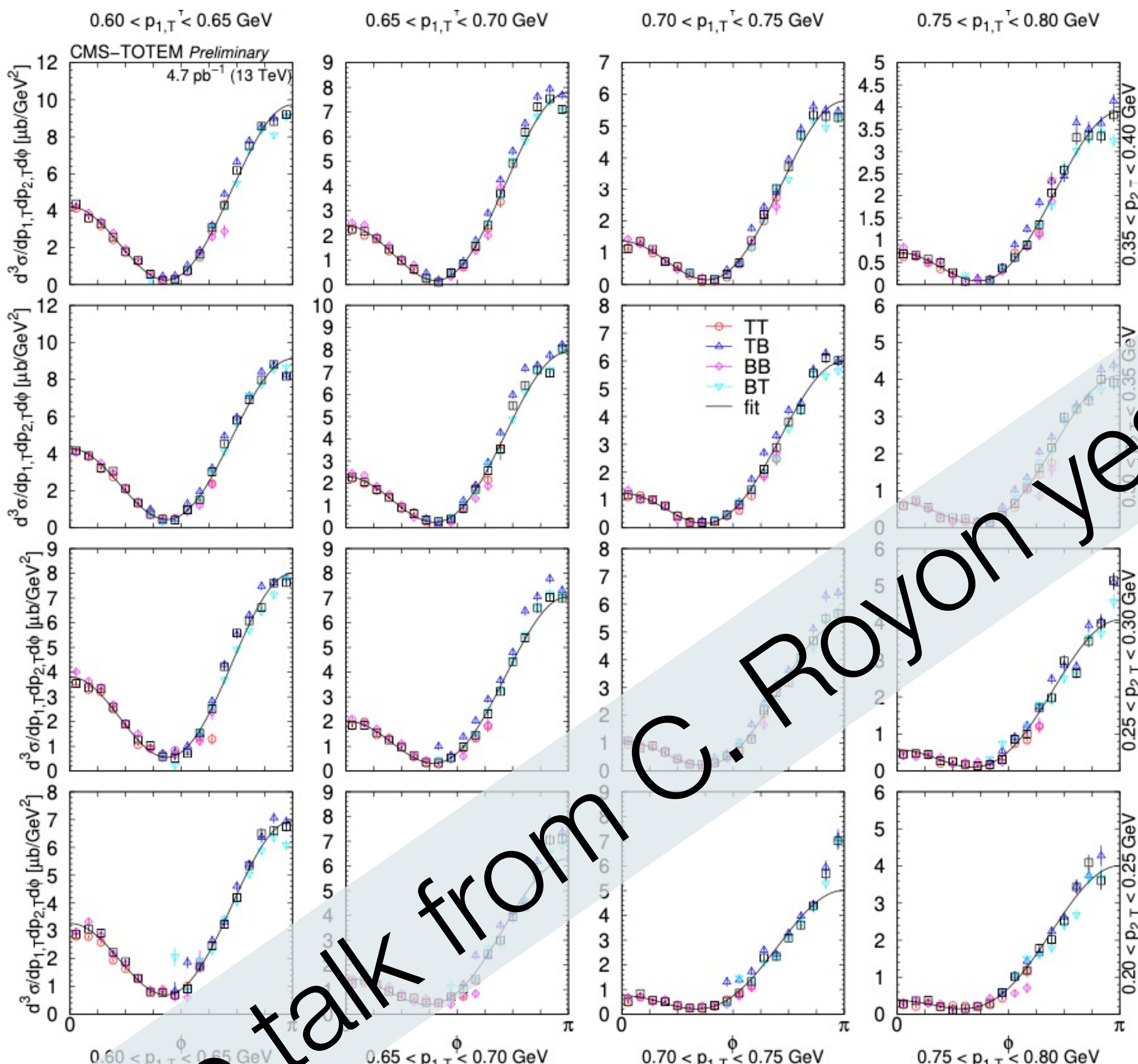

Figure 11: Distributions of $d^3\sigma/dp_{1,T}dp_{2,T}d\phi$ as a function of ϕ in the $\pi^+\pi^-$ nonresonant region $(0.35 < m < 0.65\ \text{GeV})$ in several $(p_{1,T}, p_{2,T})$ bins, in units of μb/ GeV^2. Values based on data from each RP trigger configuration (TB, BT, TT, and TT) are shown separately with coloured symbols, while the weighted average is indicated with black symbols. Results of fits with the form $[A(R - \cos\phi)]^2 + c^2$ are plotted with curves. The error bars indicate the statistical uncertainties.

ϕ= p–p azimuthal angle

π+π- pair reconstructed in the central region

Resonance-free region: $m_{\pi\pi}$<0.7 GeV and $m_{\pi\pi}$>1.8 GeV

This is just a small subset of the plots! 68 similar plots are present on the Note!

Analysis of the results

- Each distribution is fitted with: $$\frac{d^3\sigma}{\mathrm{d}p_{1,\mathrm{T}}\mathrm{d}p_{2,\mathrm{T}}\mathrm{d}\phi} = [A(R-\cos\phi)]^2 + c^2,$$
- The A, R and c dependence from t_1, t_2 are fitted with these functional forms:

$$A(t_1,t_2) = 4\sqrt{t_1 t_2}\cdot A_0 e^{b(t_1+t_2)},$$
$$R(t_1,t_2) \approx \frac{1.2(\sqrt{-t_1}+\sqrt{-t_2}) - 1.6\sqrt{t_1 t_2} - 0.8}{\sqrt{t_1 t_2}+0.1},$$
$$c(t_1,t_2) = c_0 e^{d(t_1+t_2)}.$$

See:
CMS PAS SMP-21-004
TOTEM NOTE 2023-001
for details

- Hence:

$$\frac{\mathrm{d}^3\sigma}{\mathrm{d}t_1\mathrm{d}t_2\mathrm{d}\phi} = 4\sqrt{t_1 t_2}\cdot A_0^2\cdot e^{2b(t_1+t_2)}[R(t_1,t_2)-\cos\phi]^2 + \frac{1}{4\sqrt{t_1 t_2}}\cdot c_0^2\cdot e^{2d(t_1+t_2)}, \quad (12)$$

where $A_0 = 10.6 \pm 0.2\sqrt{\mathrm{nb}}/\,\mathrm{GeV}^3$, $b = 3.9 \pm 0.1\,\mathrm{GeV}^{-2}$, while $c_0 = 2.1 \pm 0.1\sqrt{\mathrm{nb}}/\,\mathrm{GeV}$, $d = 3.8 \pm 0.1\,\mathrm{GeV}^{-2}$.

- From the fitted values, estimates of the theoretical pomeron models are extracted, in different scenarios

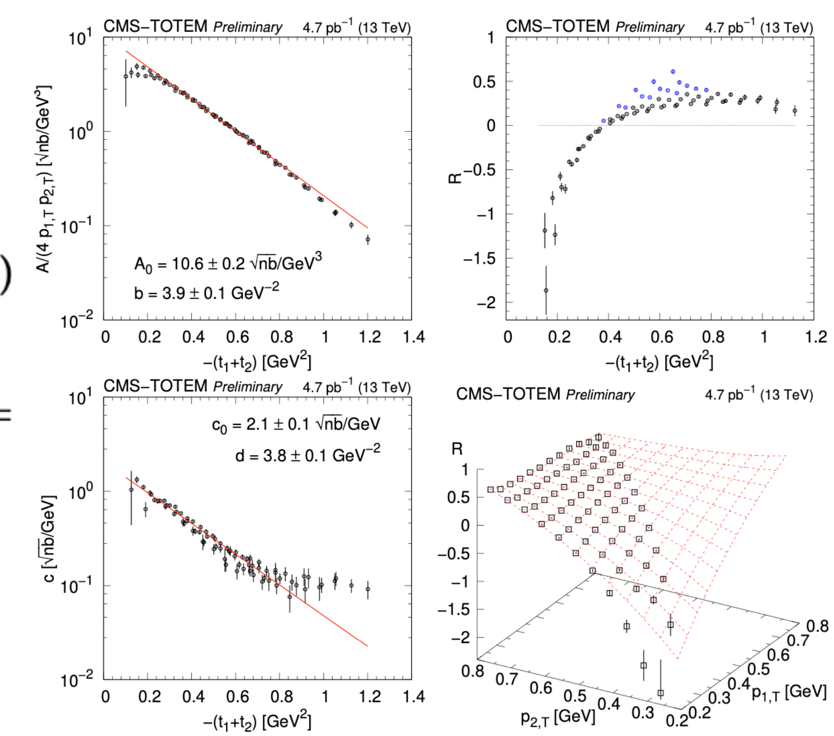

Figure 12: Dependence of the parameters A, R, and c (Eq. (8)) on (t_1, t_2). The fits correspond to the functional forms displayed in Eqs. (9)-(11). In the top right plot, points with significantly differing proton transverse momenta ($|p_{1,\mathrm{T}} - p_{2,\mathrm{T}}| > 0.35\,\mathrm{GeV}$) are coloured blue.

Conclusions

- Forward physics @LHC is a very rich field
  - Very useful info for
    - UHECR physics
    - Diffraction
    - Pomeron exchange
- Different detectors allow a very good coverage of the forward region:
  - LHCf, ZDC, Roman Pots
- Combining the central and the forward info is a real bonus!
- Different primary interactions are a wonderful opportunity
  - p-p, p-Pb, p-O for different E_{cm}

Thanks!!!

What else?

Additionally, we are able to largely expand the π^0 phase space by detecting 2 γ in the same tower (already published)

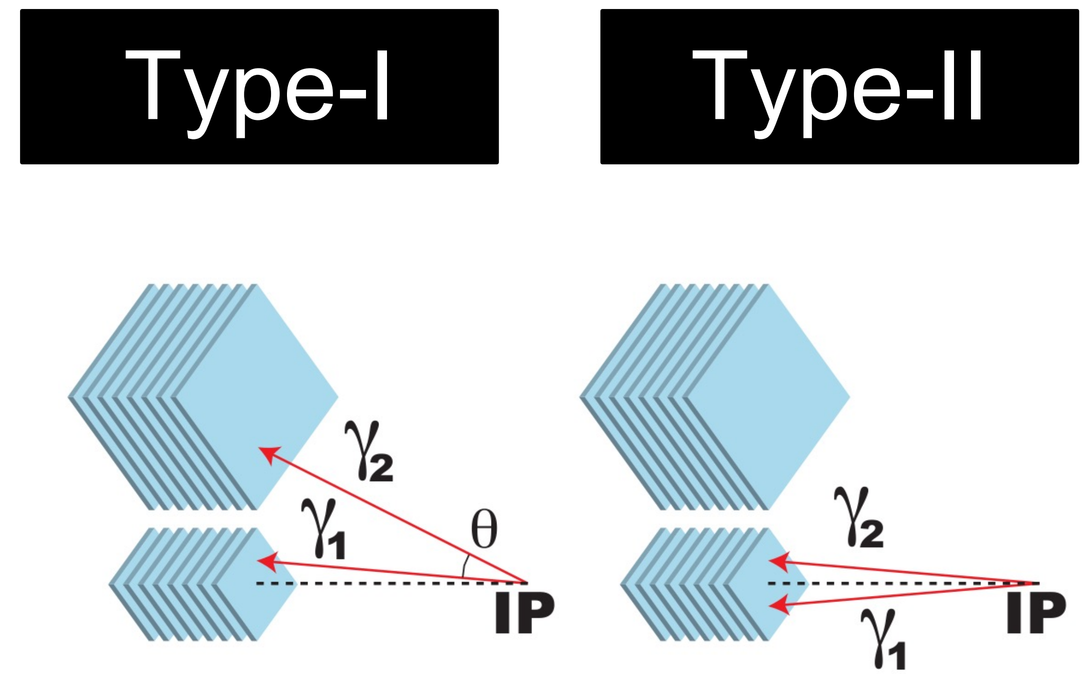

Possible future additional measurements

- 4 γ (e.g. $K^0 \rightarrow \pi^0\pi^0$)
- 1 neutron and 2 γ (e.g. $\Lambda \rightarrow n\pi^0$)

- And many possible measurements with ATLAS
  - in the central region
  - in the very forward region (Roman Pots)

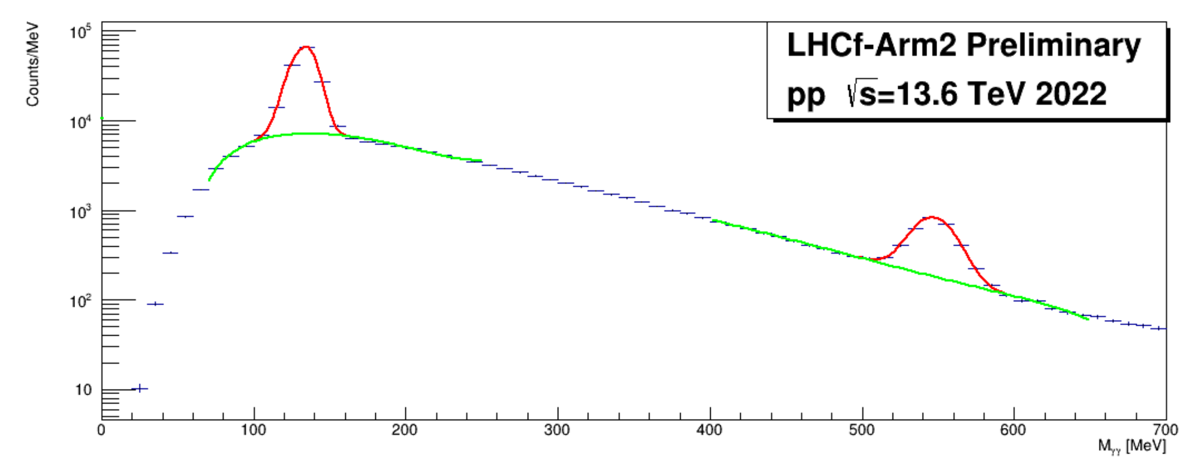

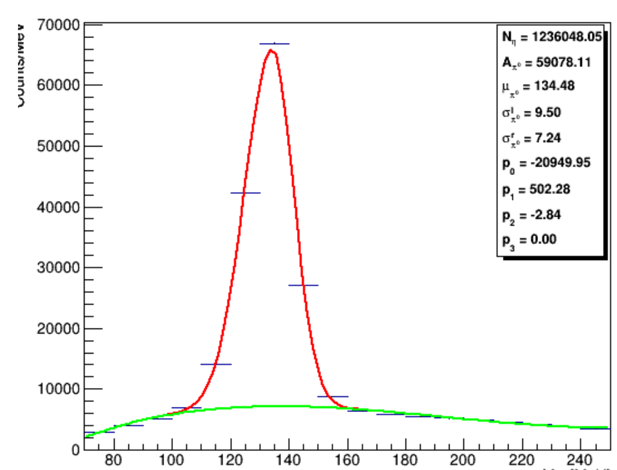

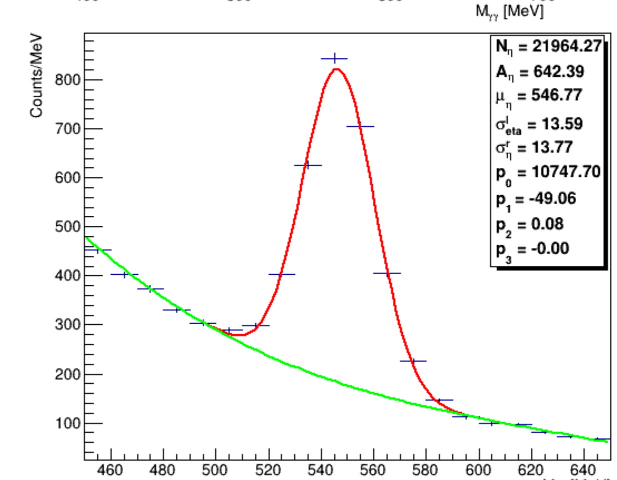

First high energy hadronic models tuning after the first LHC data (EPOS, QGSJET and SIBYLL)

Mean depth of shower maximum: Number of muons on ground:

(pre-LHC)

(post-LHC)

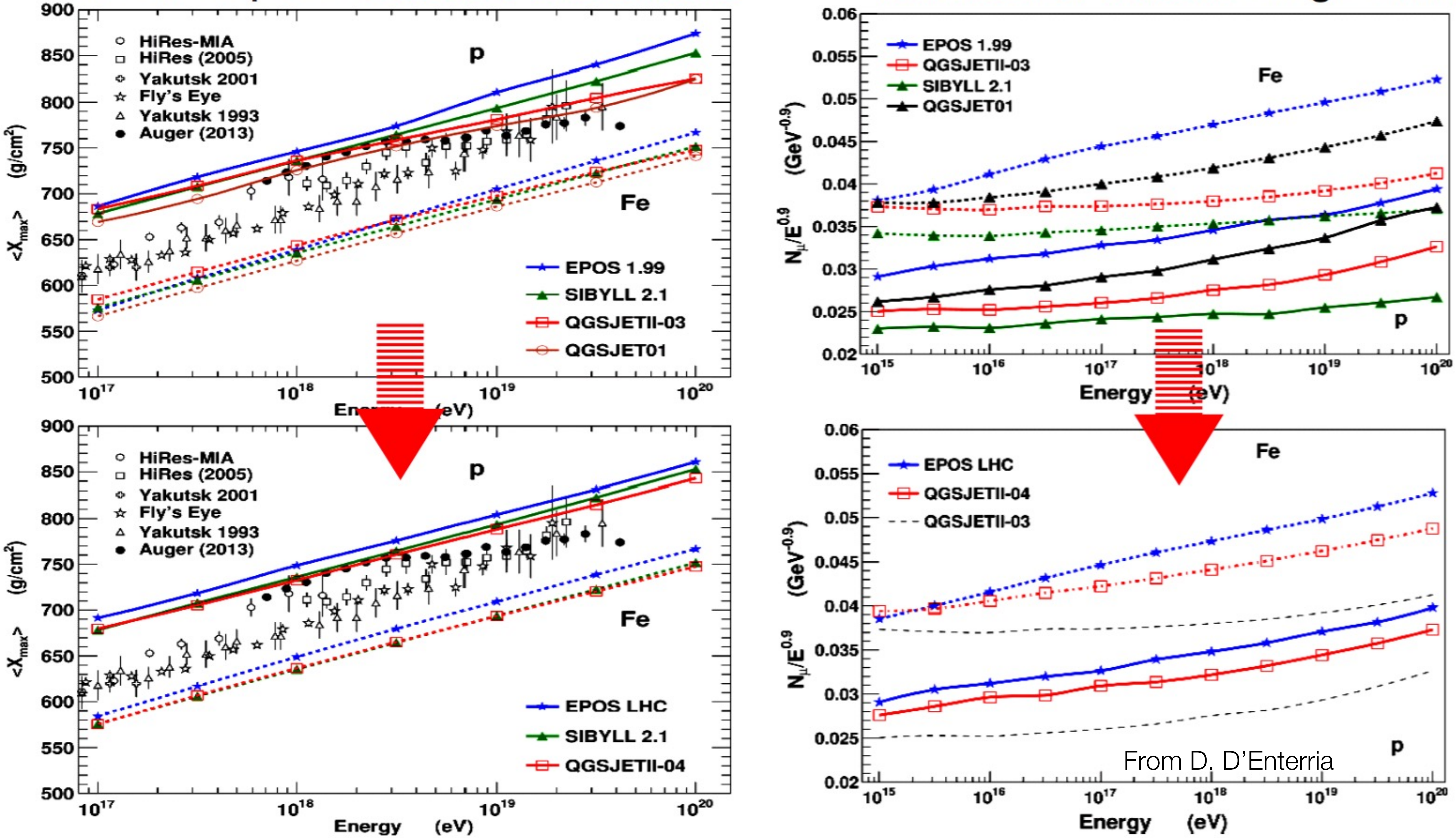

Significant reduction of differences btw different hadronic interaction models!!!
But still a lot to be done….

Hadron pairs identification

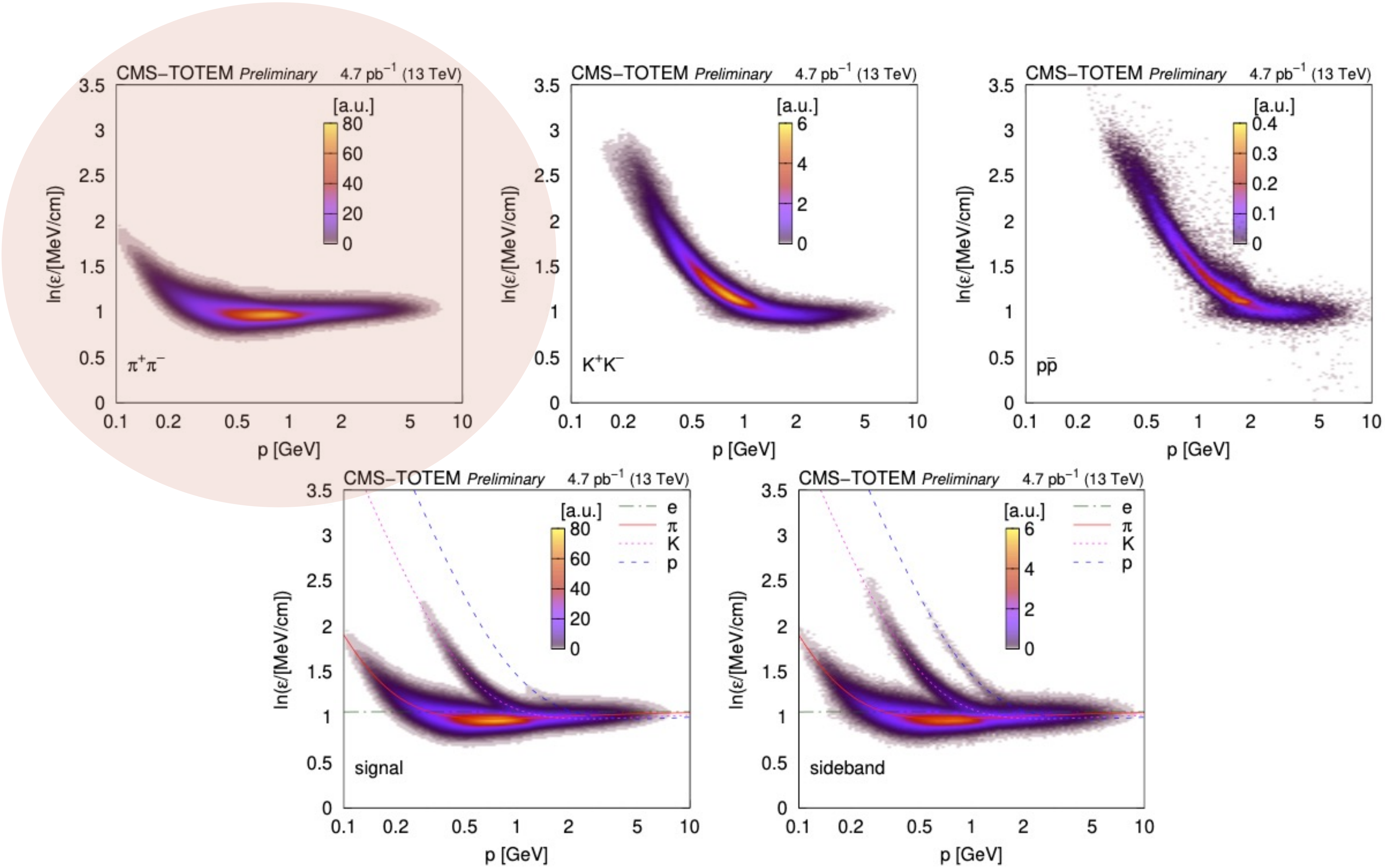

Figure 6: Distribution of $\ln\varepsilon$ as a function of total momentum, for reconstructed charged particles in selected two-track events (identified $\pi^+\pi^-$, K^+K^-, $p\bar{p}$, signal, and sideband; Section 5). The variable ε is the most probable energy loss rate at a reference path length $l_0 = 450\,\mu$m. The colour scale is shown in arbitrary units and is linear. The curves show the expected $\ln\varepsilon$ for electrons, pions, kaons, and protons (Eq. (34.12) in Ref. [1]).

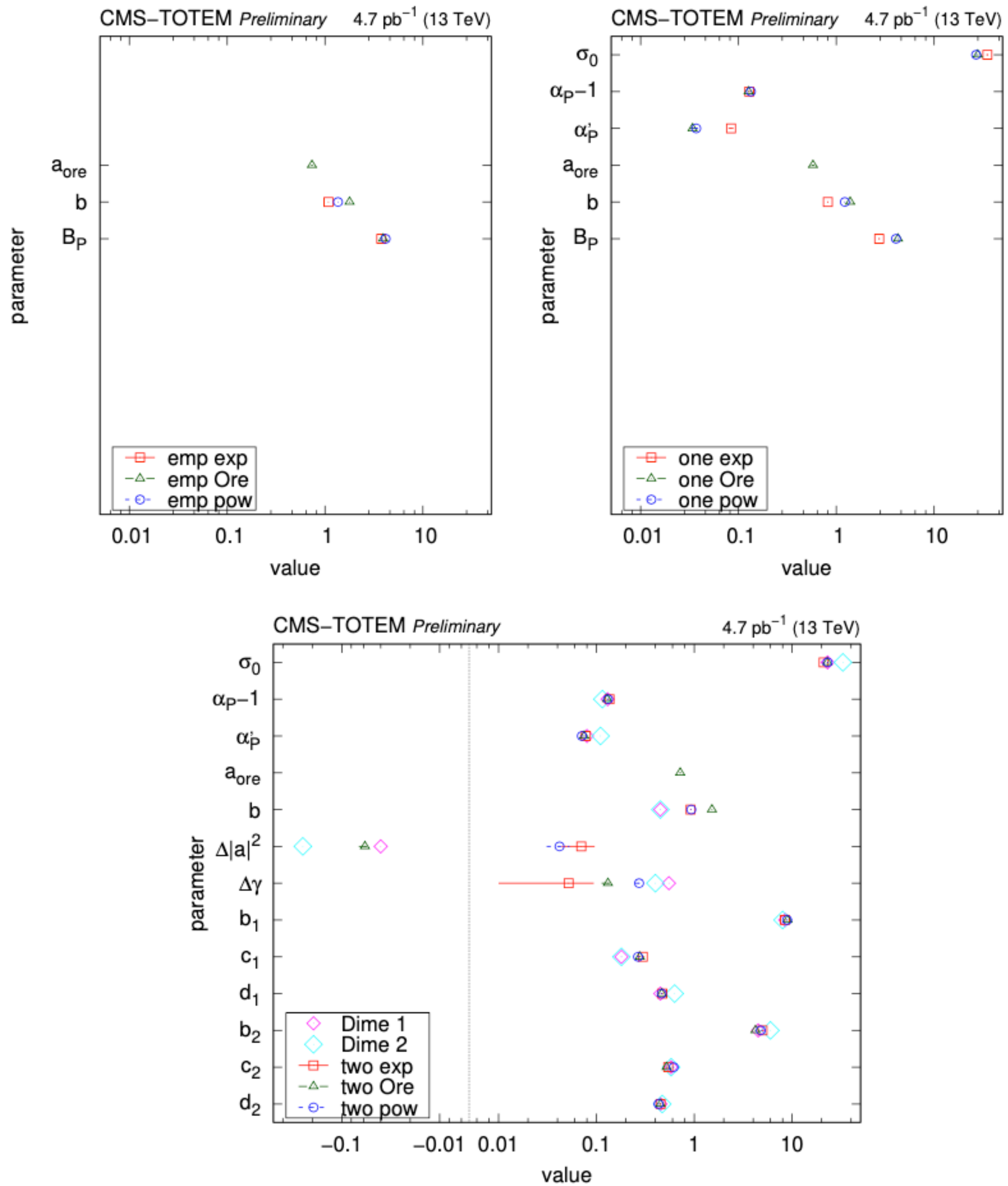

Figure 13: Values of best parameters for the empirical (top left), one-channel (top right), and two-channel (bottom) models with several choices of the proton-pomeron form factor (exponential, Orear-type, power-law). In the case of the two-channel model, parameter values of models describing the elastic differential proton-proton cross section from Ref. [26] are also indicated (DIME 1 and 2).

Diffractive and non-diffractive production

√s = 13 TeV - η > 10.94

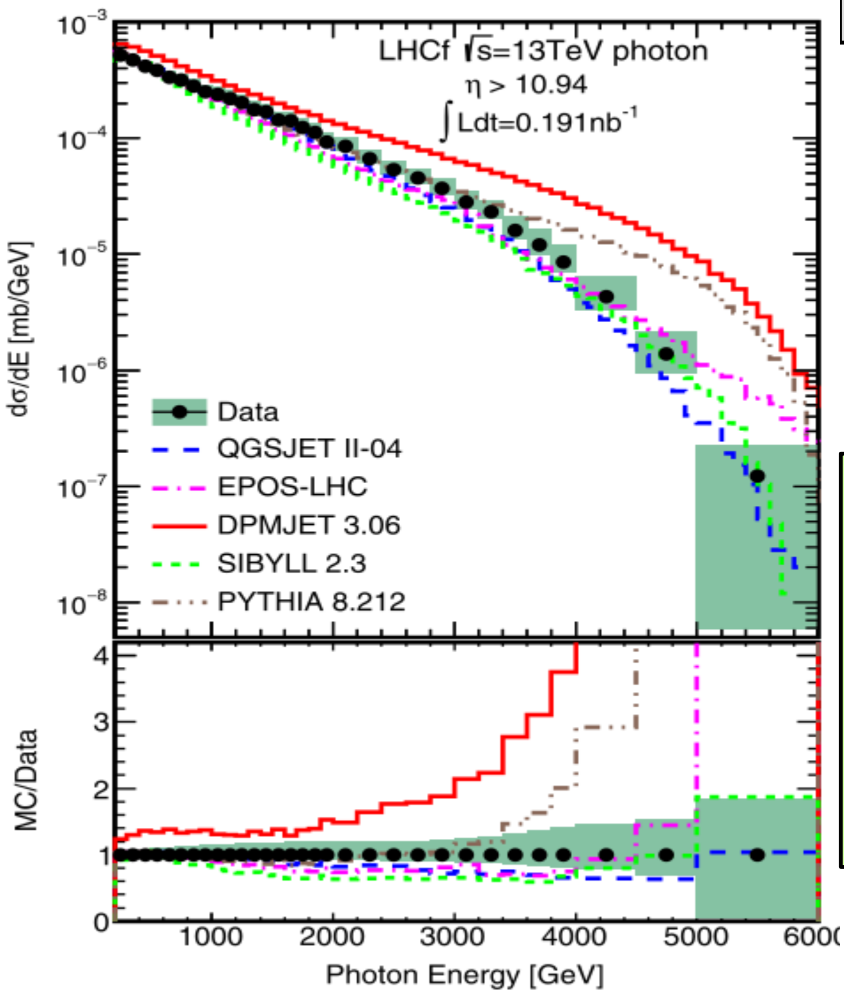

Different models lead to different contributions to **diffractive** and **non-diffractive** events

How to separate diffractive and non-diffractive production?

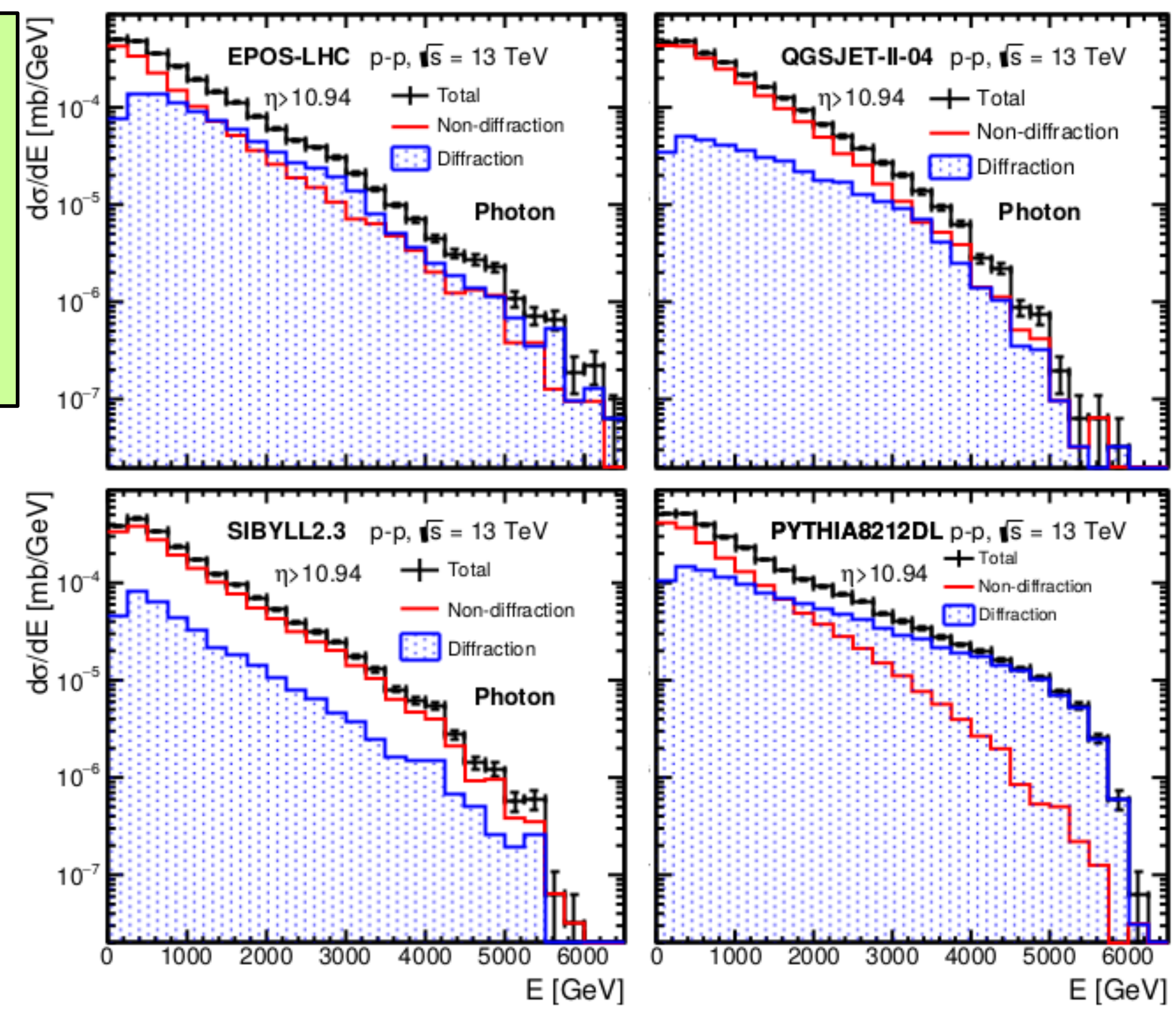

LHCf measures the **total production rate** in the forward region

LHCf-ATLAS joint analysis

Eur. Phys. J. C (2017) 77:212

π^0 Production Rate
p-p $\sqrt{s}$ = 13 TeV

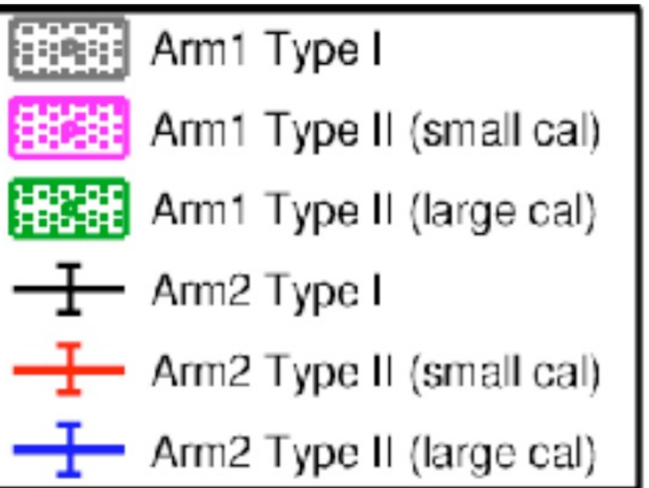

Ongoing analysis

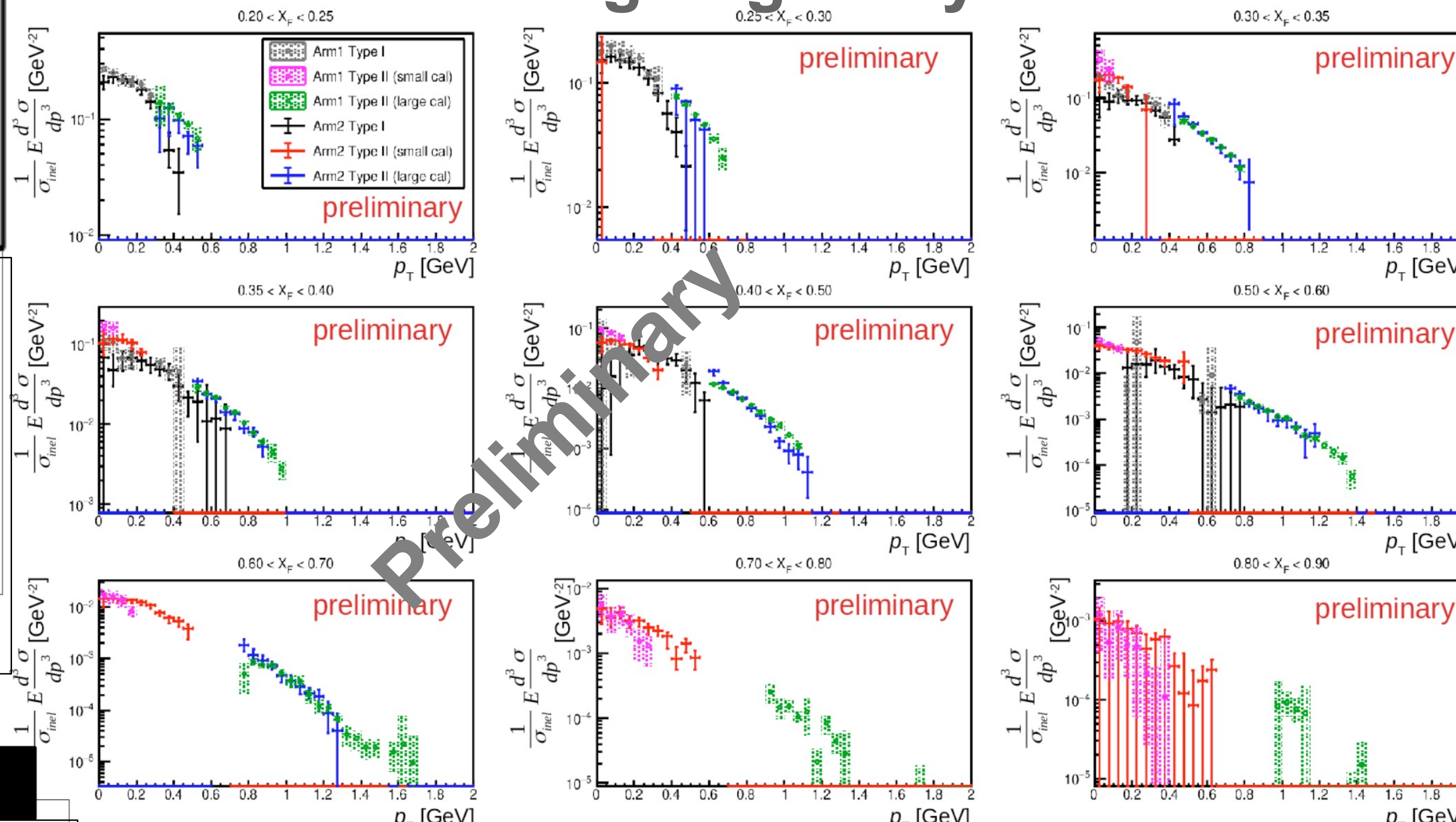

Different Arm1 and Arm2 geometries allows for a large **<u>p_T vs x_F coverage</u>** with <u>an overlap to crosscheck results</u>

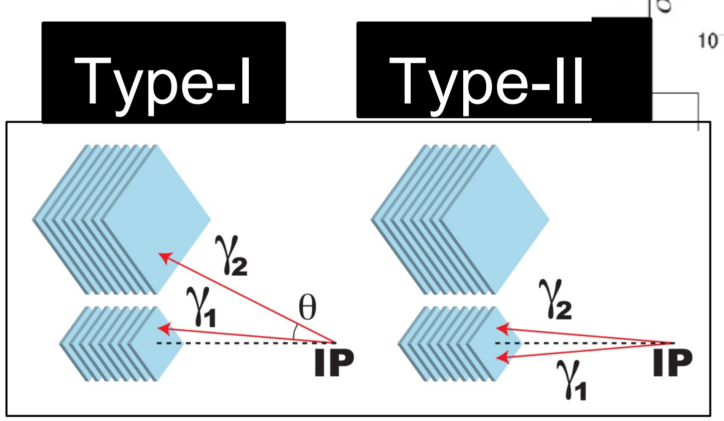

Good *agreement* between Arm1 and Arm2 data and between "Type-I" and "Type-II" events

π^0@5.02 TeV p-Pb: Nuclear Modification Factor

PhysRevD.94.032007

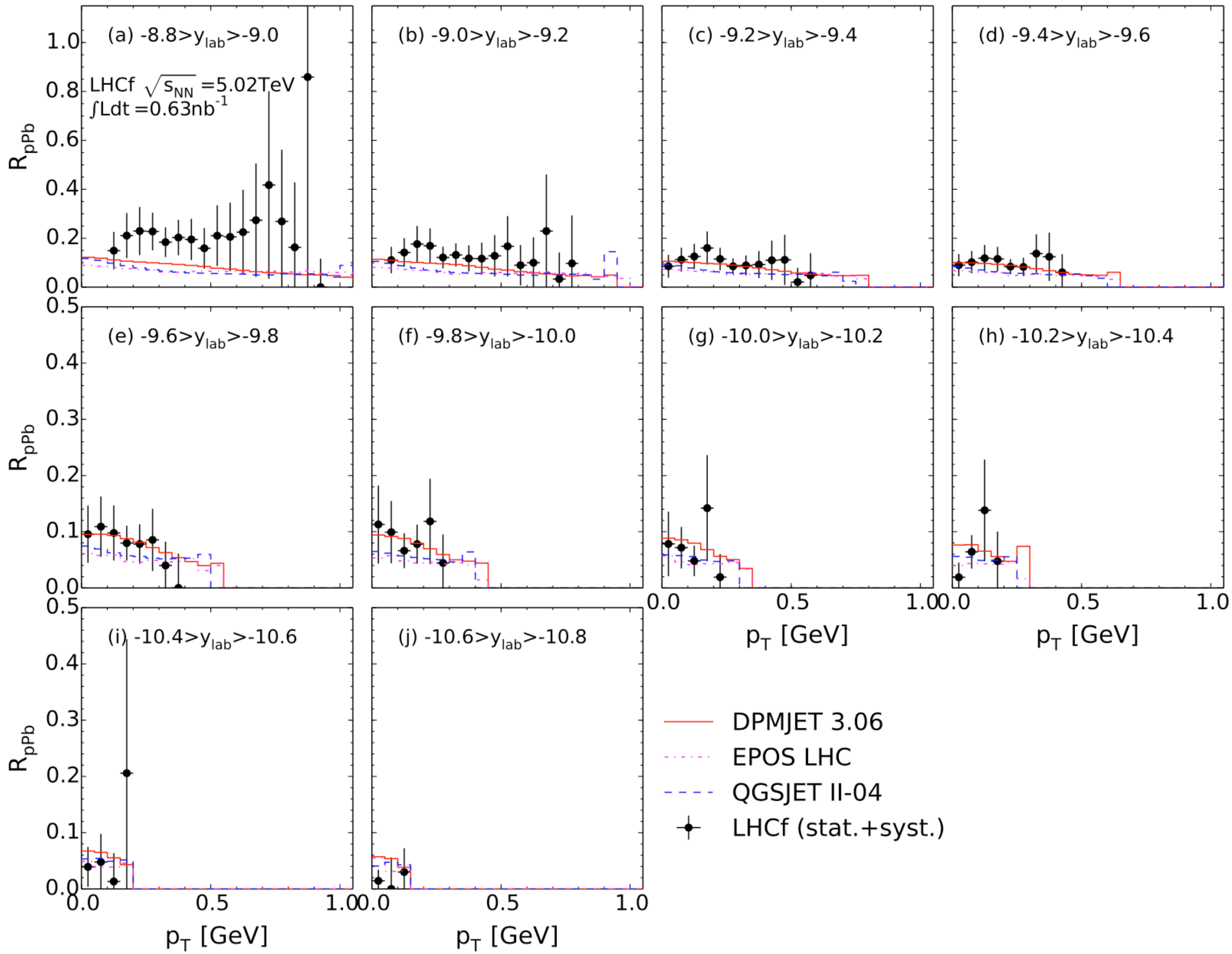

Neutrons@13 TeV: spectra

JHEP07(2020)016

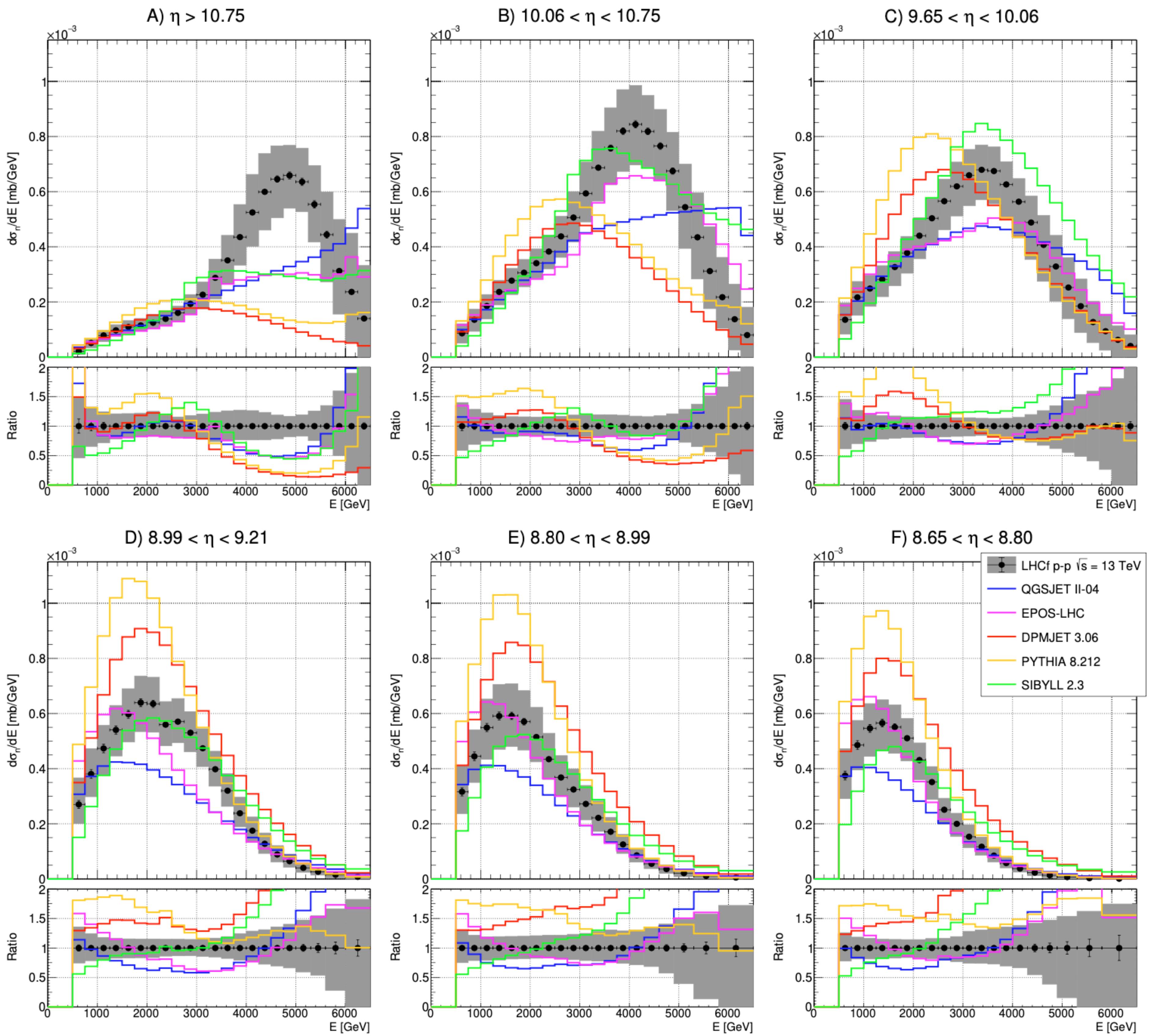

Neutrons@13 TeV: Energy Flow

JHEP07(2020)016

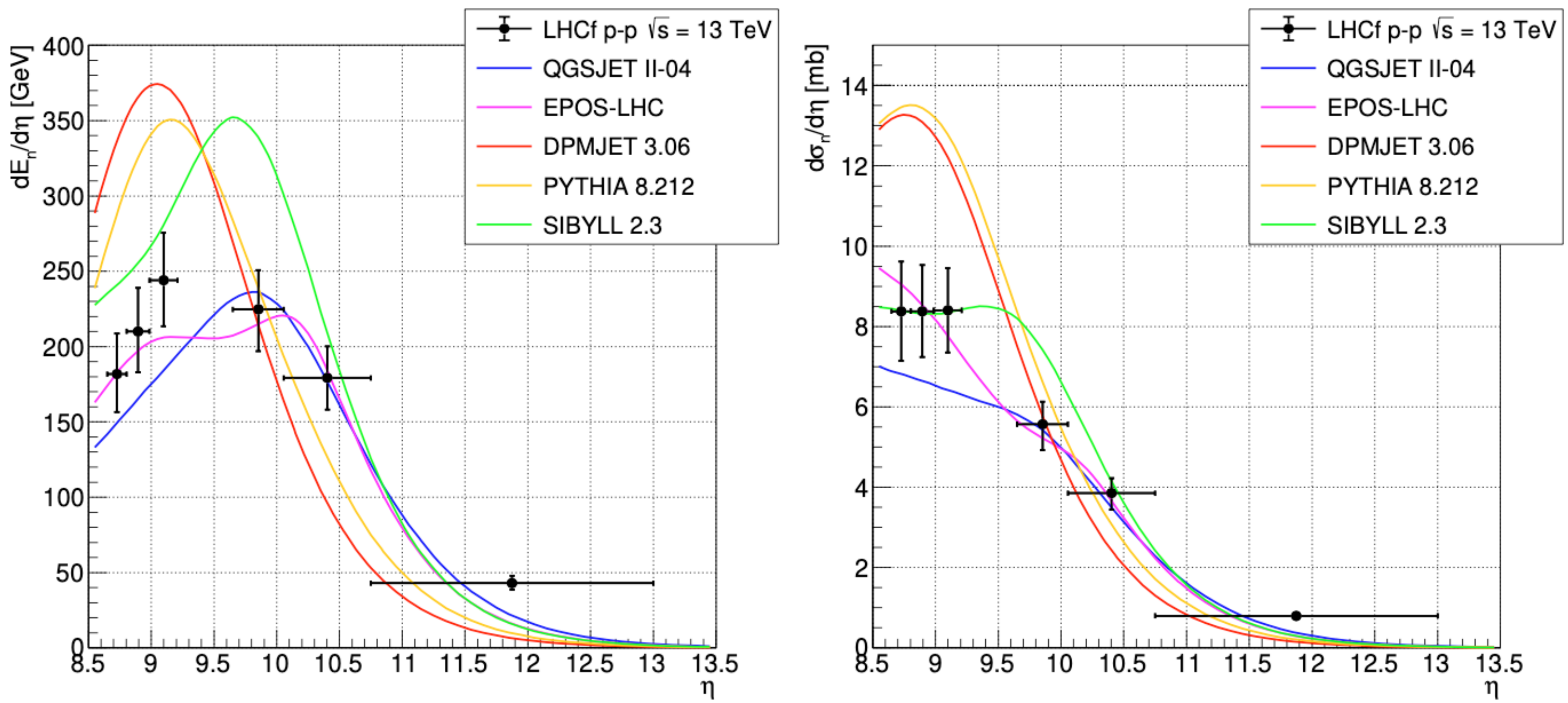

Figure 3. Differential energy flow $\mathrm{d}E_\mathrm{n}/\mathrm{d}\eta$ (left) and differential cross section $\mathrm{d}\sigma_\mathrm{n}/\mathrm{d}\eta$ (right) of neutrons produced in p-p collisions at $\sqrt{s} = 13\,\mathrm{TeV}$, measured using the LHCf Arm2 detector. Black markers represent the experimental data with statistical and systematic uncertainties, whereas colored lines refer to model predictions at the generator level.

LHCf @ pPb 5.02 TeV and 8.16 TeV

(Soft) QCD :

central and peripheral collisions

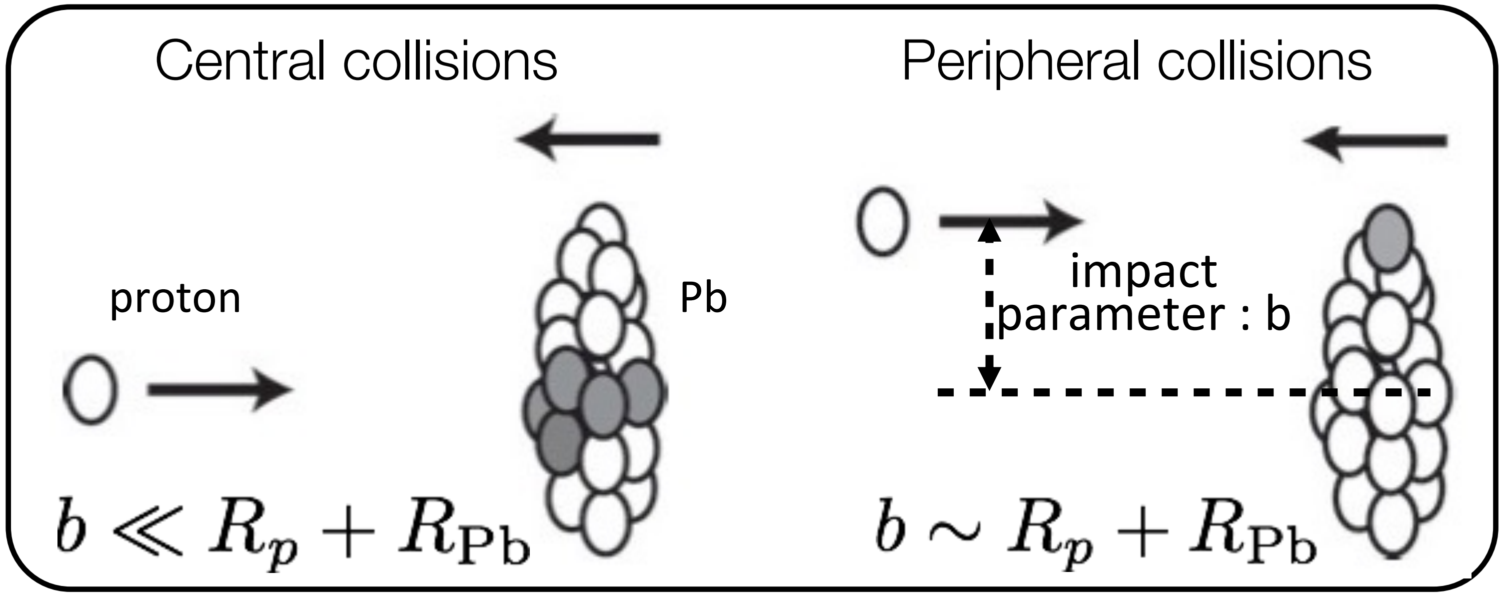

Ultra peripheral collisions :

virtual photons from rel. Pb collides a proton

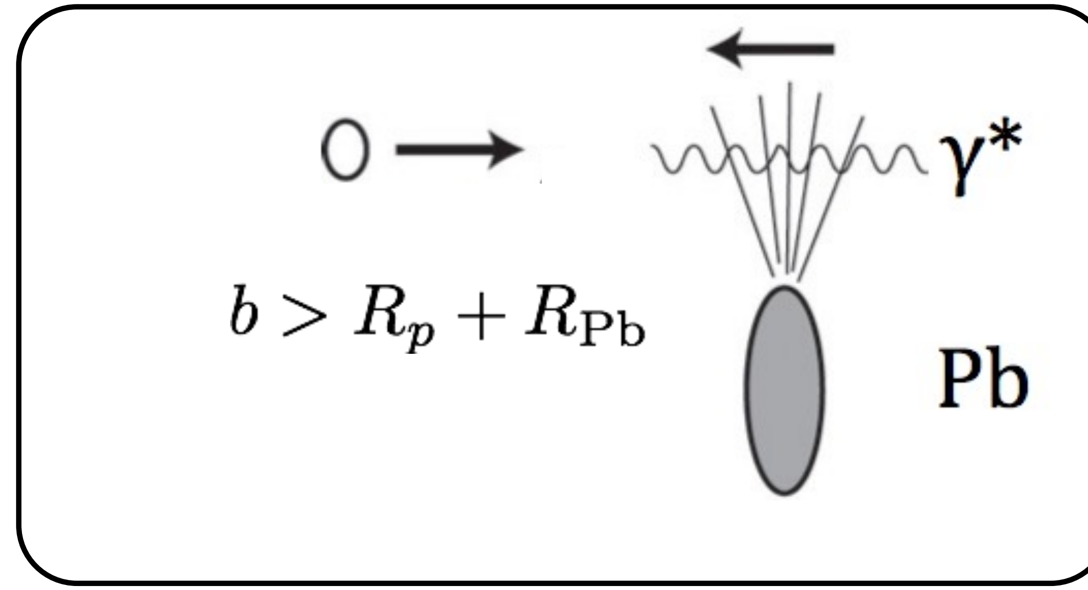

proton rest frame

Momentum distribution of the UPC induced secondary particles is estimated as

1. energy distribution of virtual photons is estimated by the Weizsacker Williams approximation.
2. photon-proton collisions are simulated by the SOPHIA model (E_γ > pion threshold).
3. produced mesons and baryons by γ-p collisions are boosted along the proton beam.

Dominant channel to forward π^0 is

$$\gamma + p \rightarrow \Delta(1232) \rightarrow p + \pi^0$$

About half of the observed π^0 may originate in UPC, another half is from soft-QCD.

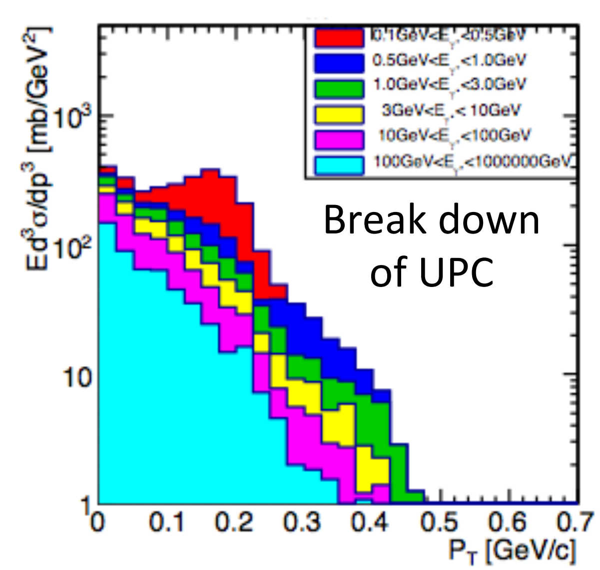

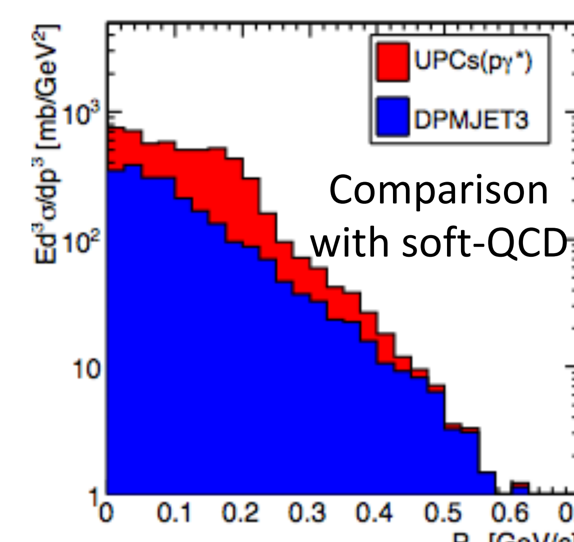

π^0 in p+p @ 13 TeV

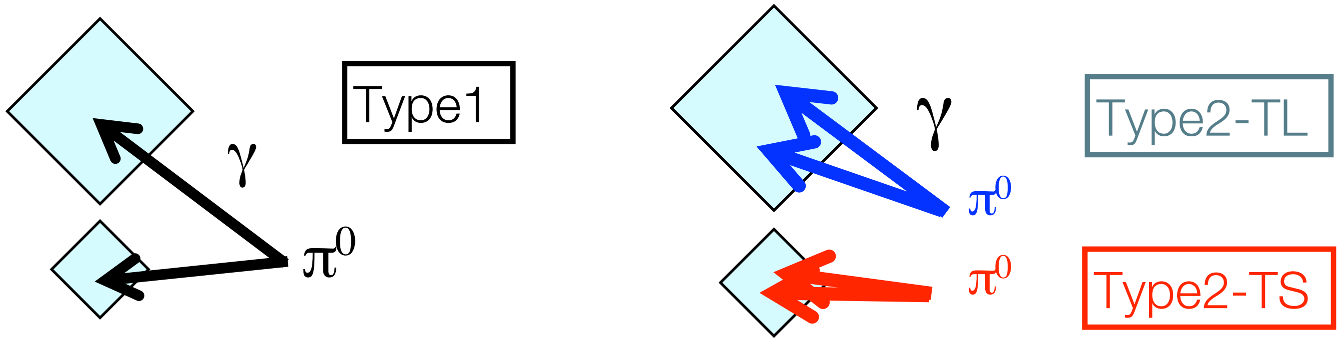

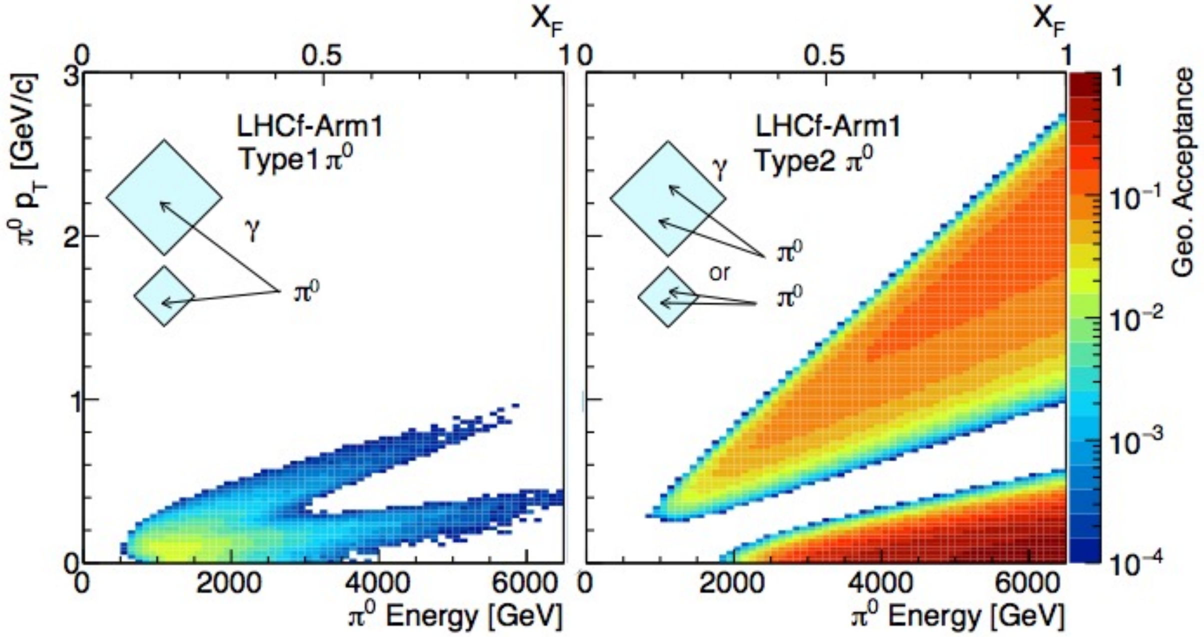

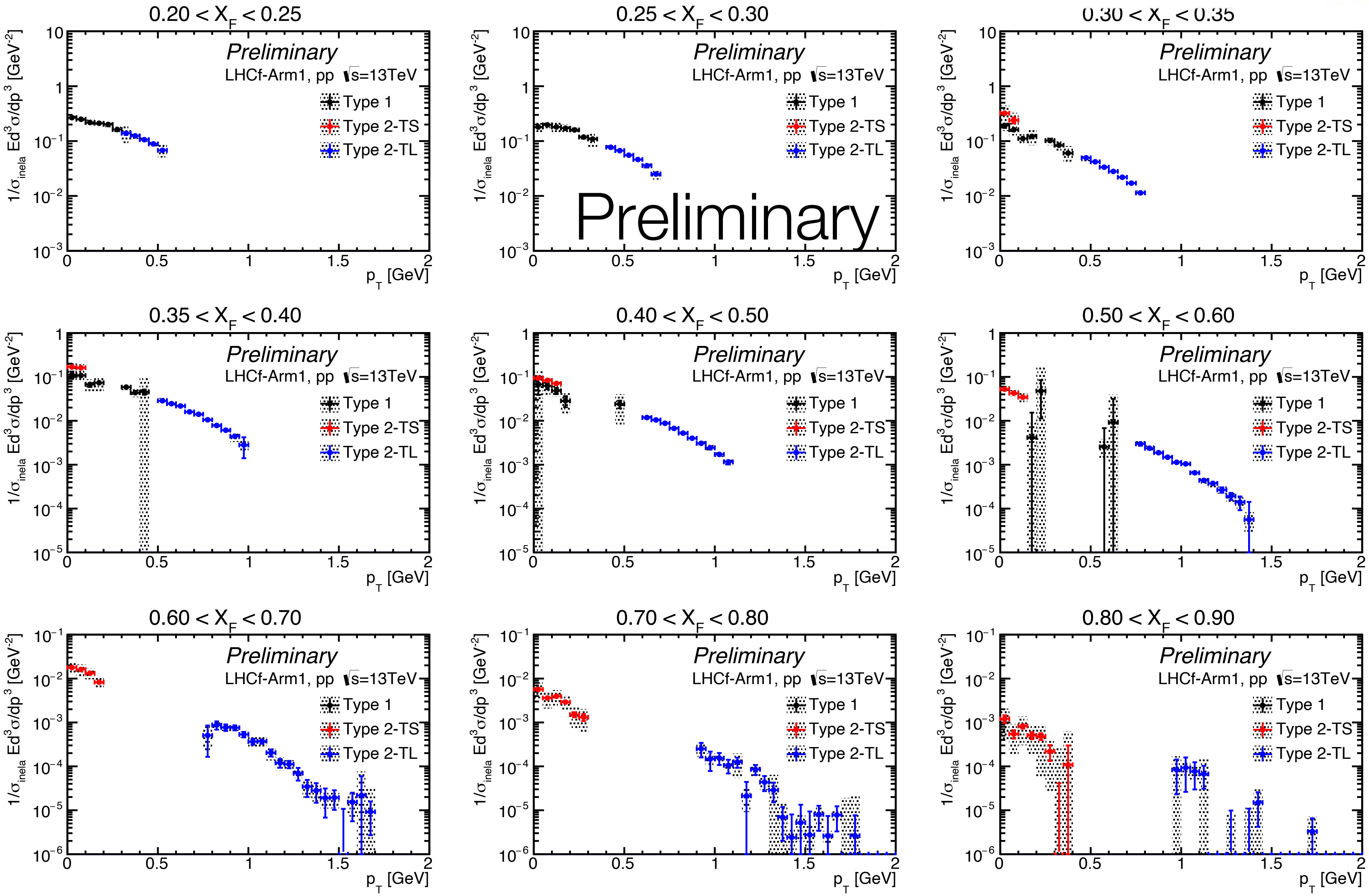

- Smooth connection of 3 spectra
- Wide transverse momentum coverage
- The gaps will be covered by Arm2 and other detector position data.

Measurement of interesting quantities for CR Physics

Inelasticity VS θ

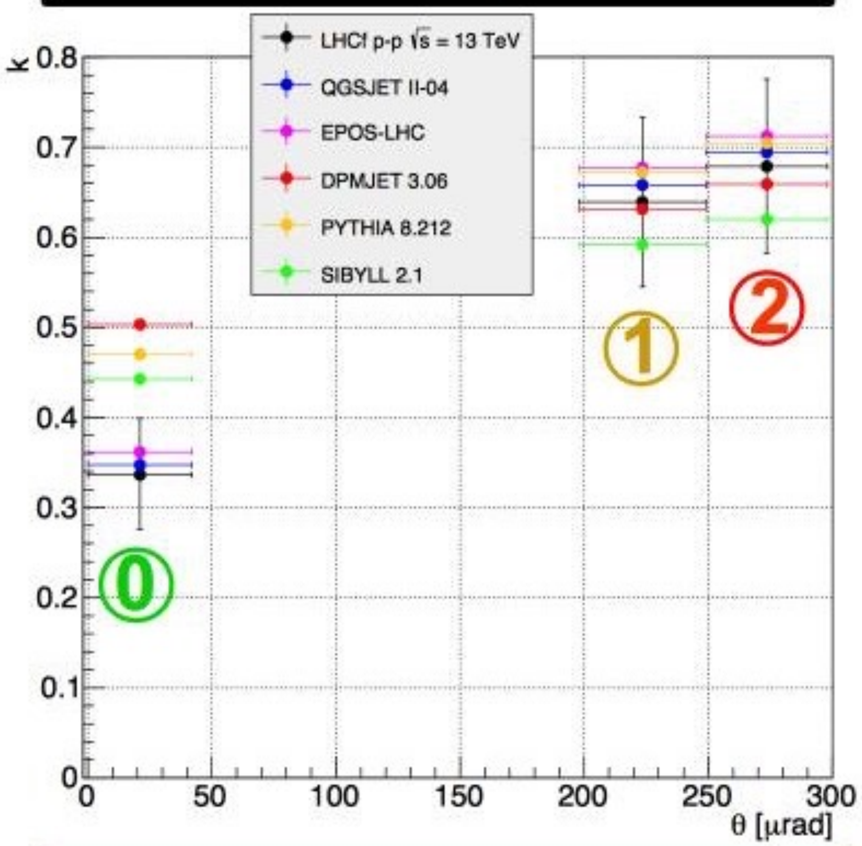

All models overestimate inelasticity in the most forward region even if **QGSJET II-04** and **EPOS-LHC** are consistent within the error bars

dσ/dη VS η

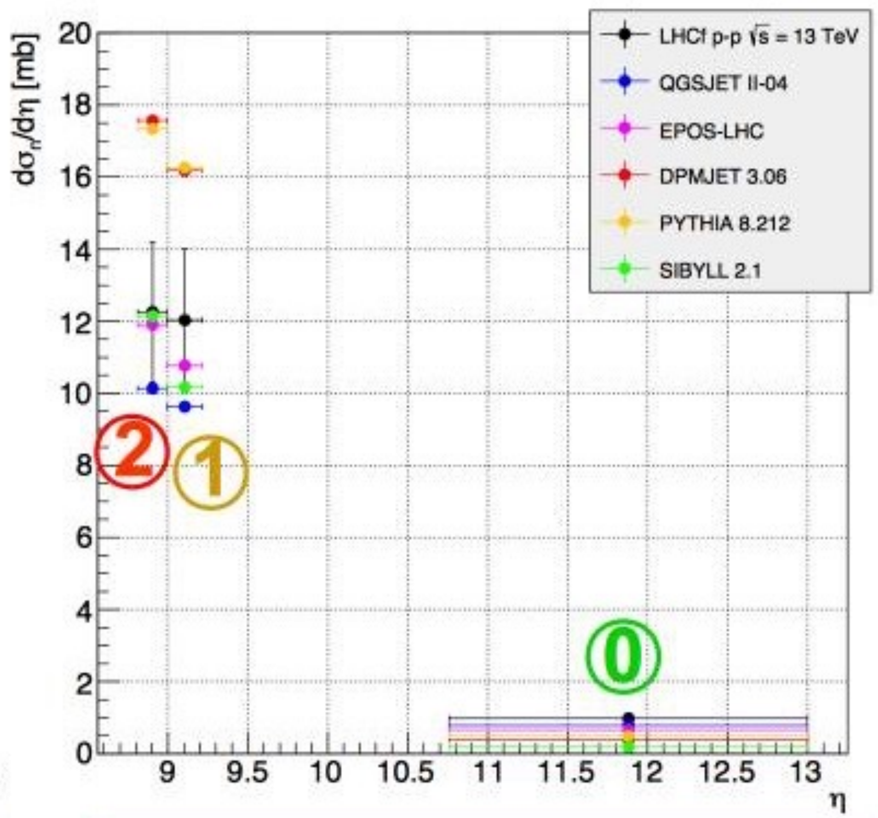

EPOS-LHC and **SIBYLL 2.1** reproduce enough well the measured total differential cross section except in the most forward region

dE/dη VS η

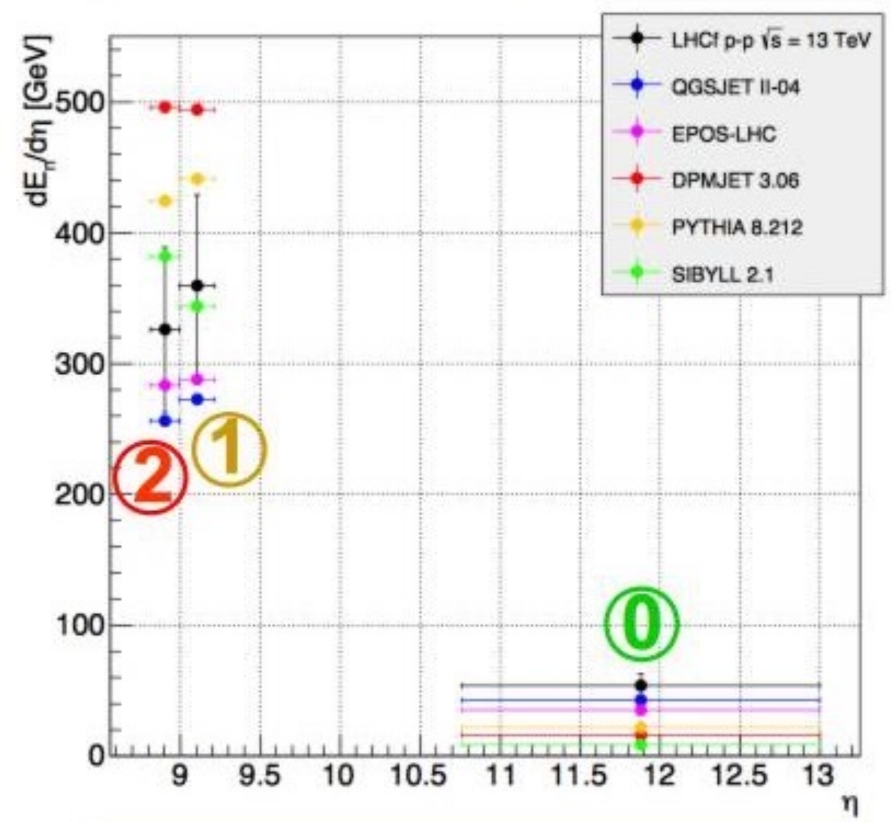

Where the energy flux is high, the agreement between experimental measurements and **SIBYLL 2.1**/**EPOS-LHC** is quite good

π^0 reconstruction

Longitudinal development measured by scintillator layers

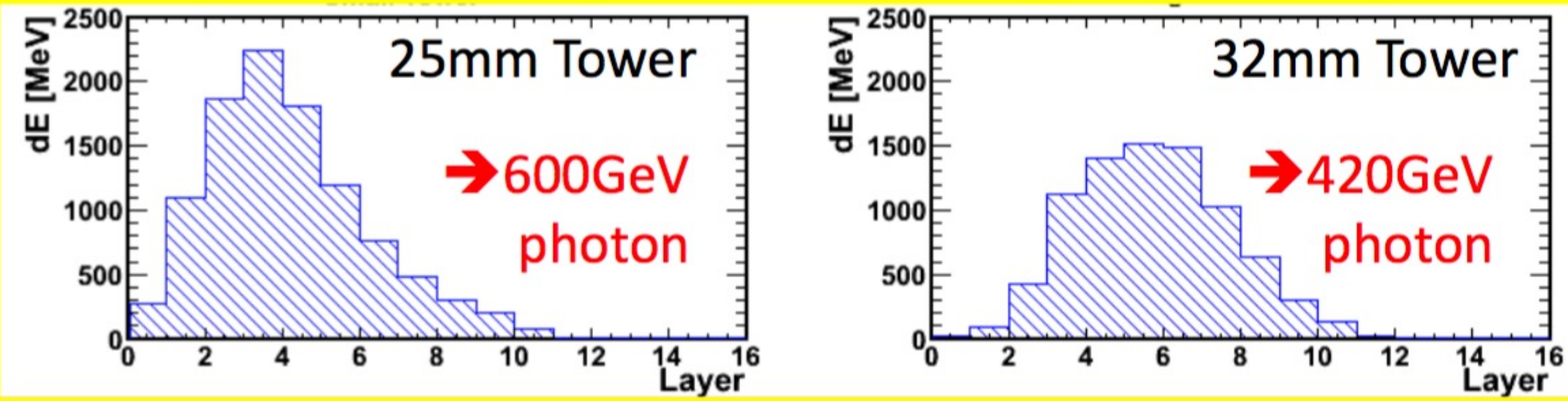

Determination of **energy** from total energy release

PID from shape

Transverse profile measured by silicon μ–strip layers

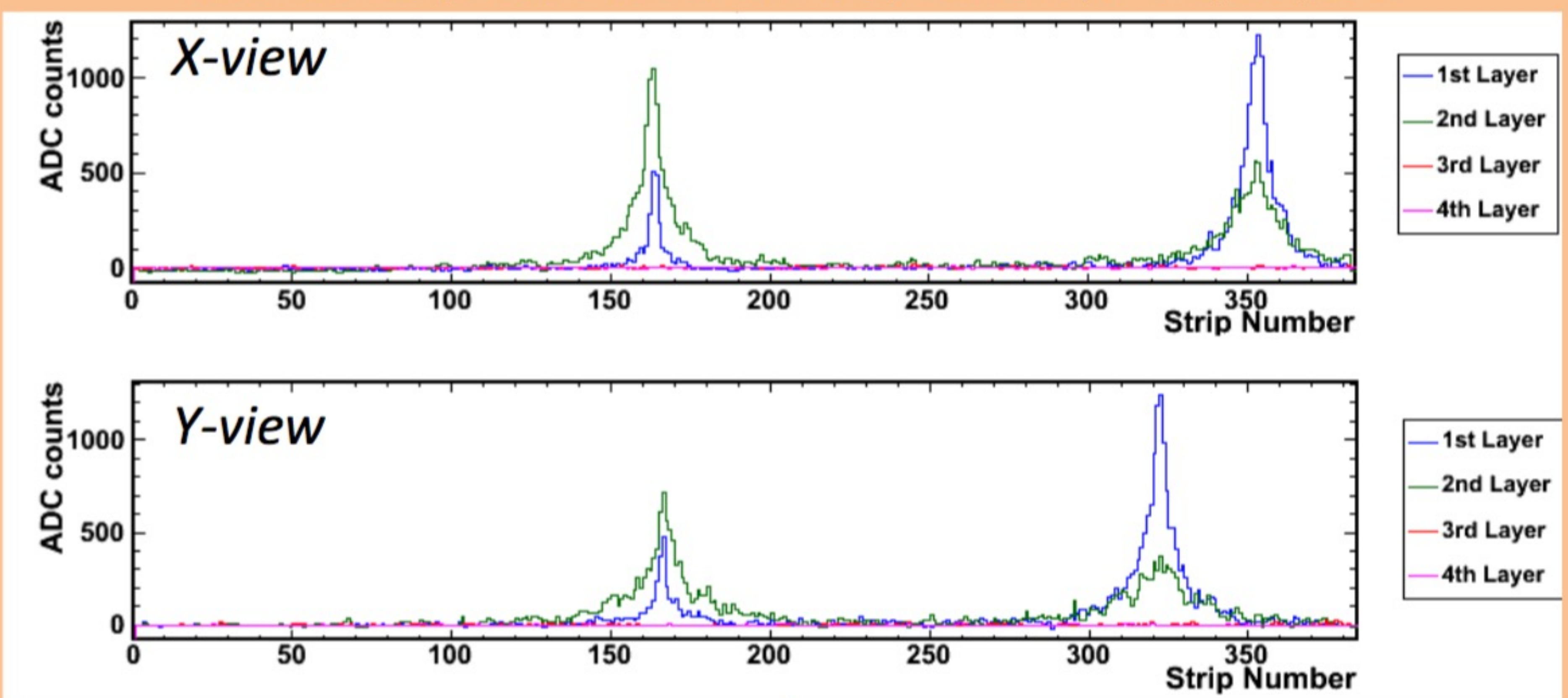

Determination of the **impact point**

Measurement of the **opening angle** of gamma pairs

Identification of **multiple hit**

LHCf π^0 results: improvement @ 7 TeV

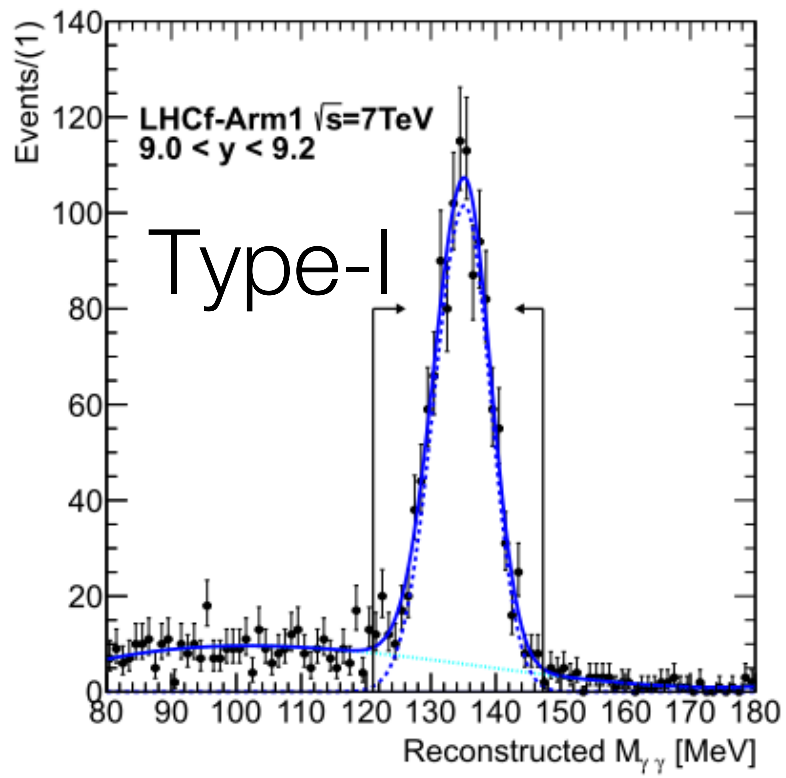

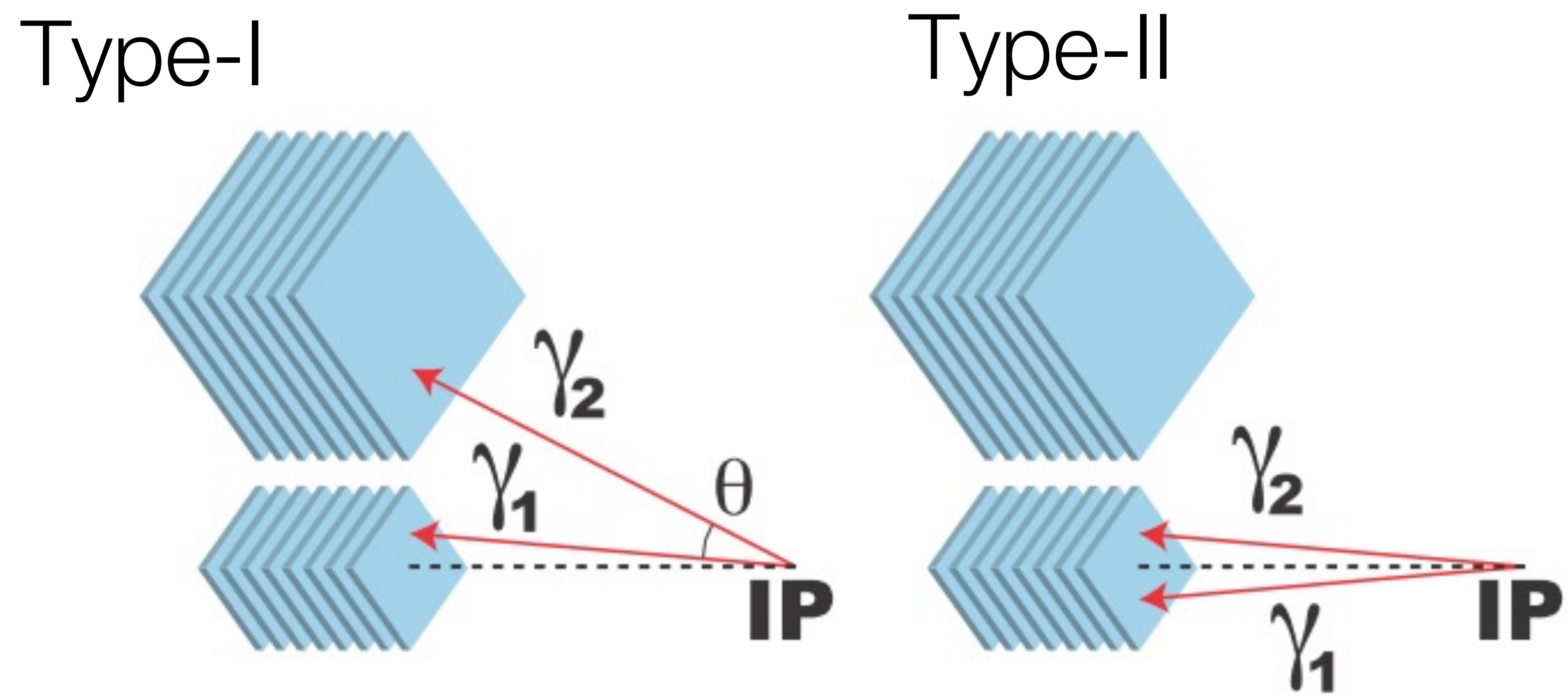

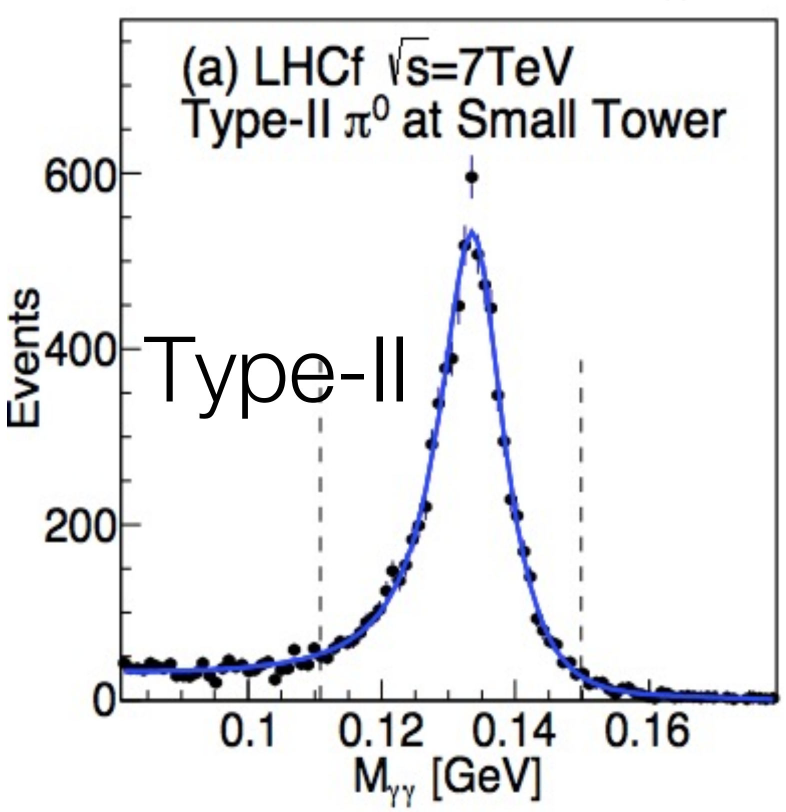

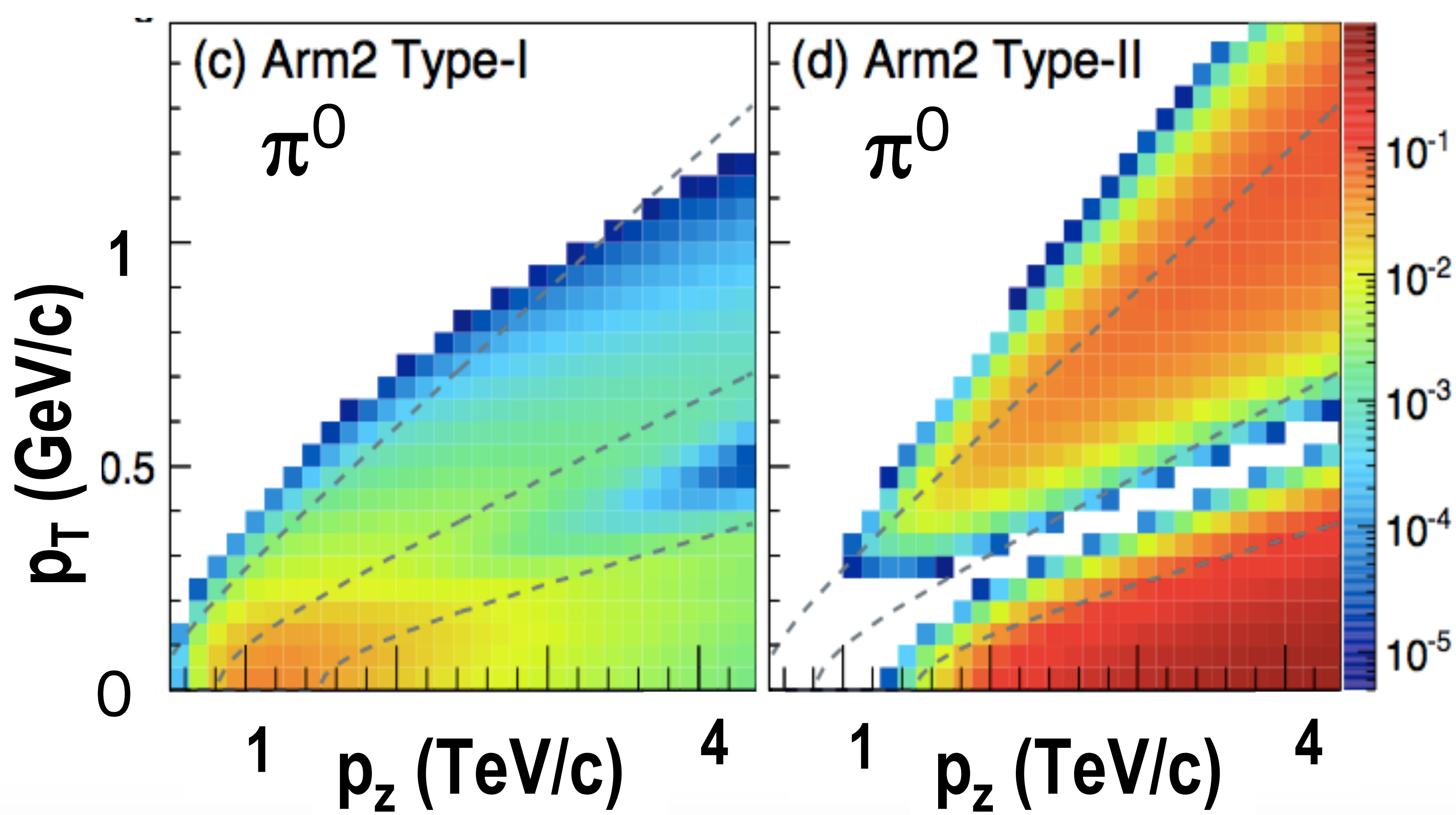

LHCf neutron analysis: motivations

Inelasticity measurement $k=1-p_{leading}/p_{beam}$

Muon excess at Pierre Auger Observatory

- cosmic rays experiment measure PCR energy from muon number at ground and florescence light
- 20-100% more muons than expected have been observed

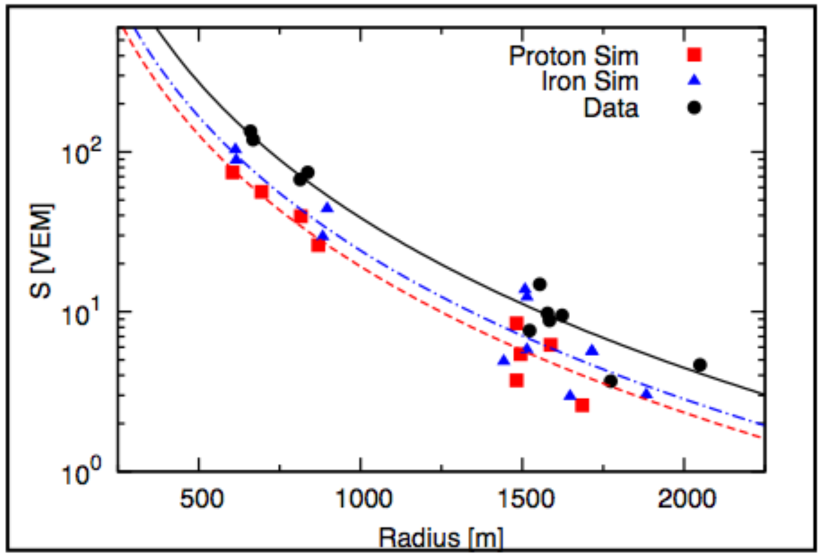

[J.Allen, et al. ICRC2011 Proceedings]

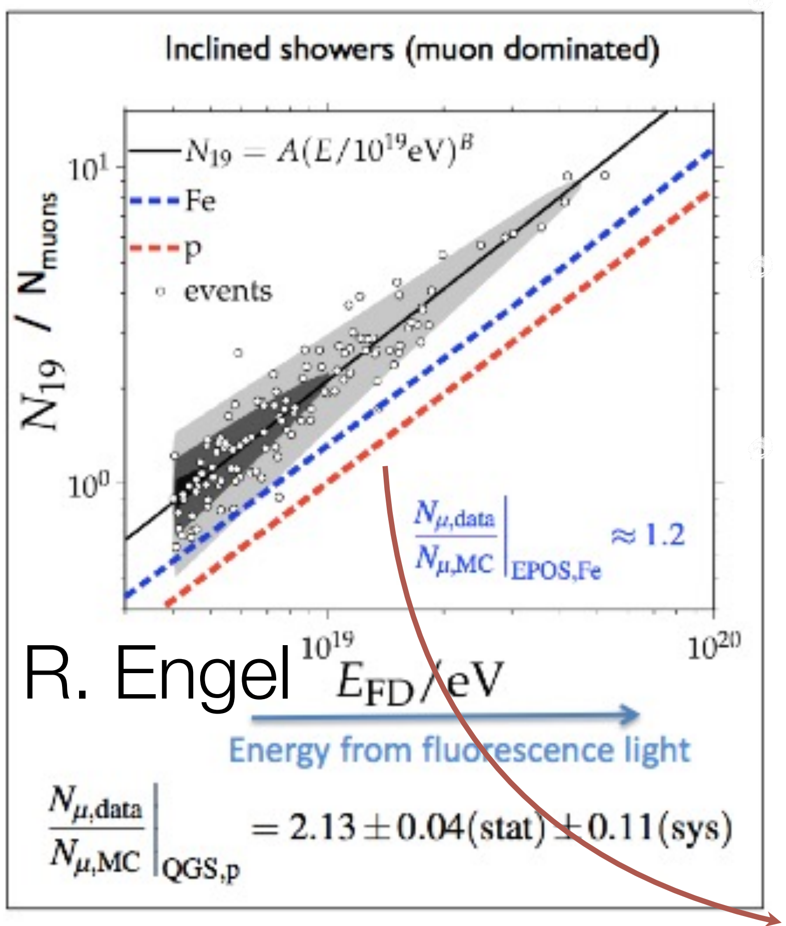

Number of muons depends on the energy fraction of produced hadron

Muon excess in data even for Fe primary MC

EPOS predicts more muon due to larger baryon production

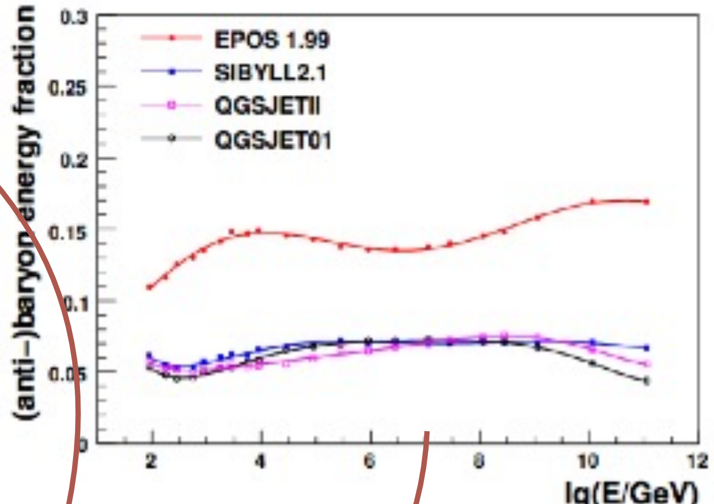

Neutron spectra predicted by interaction models

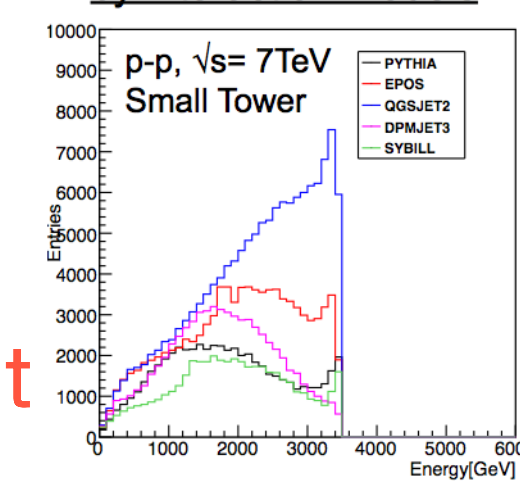

importance of baryon measurement